



**Republic of Iraq**  
**Ministry of Higher Education  
and Scientific Research**  
**University of Baghdad**  
**Institute of Laser for  
Postgraduate Studies**



# **Effect of Yb Fiber Laser on Bonding of Resin Cement Retained Titanium Implant Dental Abutment**

A Thesis Submitted to the Institute of Laser for Postgraduate Studies,  
University of Baghdad in Partial Fulfillment of the Requirements for  
the Degree of Master of Science in Laser / Dentistry

**By**

**Ruba Husam Abdulrazzaq**

B.D.S. 2012

**Supervisor**

**Asst. Prof. Dr. Basima Mohammed Ali Hussien**

B.D.S, M.Sc, Ph.D.

**2022 A.D.**

**1443 A.H.**

بِسْمِ اللَّهِ الرَّحْمَنِ الرَّحِيمِ

وَفَوْقَ كُلِّ ذِي عِلْمٍ عَلِيمٌ

صَدَقَ اللَّهُ الْعَظِيمُ

سورة يوسف الآية رقم { ٧٦ }

## **ACKNOWLEDGMENT**

At first, Many thanks with all respect to **Prof. Dr. Hussein A. Jawad**, Dean of the Institute of Laser for Postgraduate Studies, for his great helping and continuous support during the period of search.

I would like to give special thanks to my supervisor **Asst. Prof. Dr. Basima Mohammed Ali** (Institute of Laser for Postgraduate studies), for suggesting this work, her guidance, encouragement and support have definitely had a substantial impact on this work.

Special thanks with all respect to **Dr. Layla AL-Amirry**, Head of the medical and biological Applications, for her helping during the study.

I would also like to show gratitude to all the teaching staff of Institute of Laser for Postgraduate Studies, including (**Prof. Dr. Abdul-Hadi M. AlJanabi, Asst. Prof. Dr. Zeyad A. Taha and Asst. Prof. Dr. Mohammed Kareem Daher**) for their grateful remarks and advices during the period of search.

I acknowledge to **Eng. Atheer Rasheed** (Institute of Laser for Postgraduate Studies) for his great helping.

Finally, I would like to thank my colleagues in the institute for their great help and for being by my side.

## **DEDICATION**

*To my great father whom I'm proud of carrying his  
name*

*To my great mother who made me what I am today*

*To my Wonderful brothers and sister who support  
me every time*

*To my little angel Noor who make the meaning to  
my life.*

*Ruba*

## Abstract

**Background:** Retention between implant abutment and resin cement is one of the major factors that contribute to the longevity of the implant-supported restorations. This retention is affected mainly by some factors including surface features for example surface area and surface roughness. Surface modification of implant abutment could be achieved by several methods such as sandblasting, grinding, acid etching, and laser treatment. With advancement in technology, lasers have been used for titanium surface modification because they are highly efficient and easily used.

**Aim:** to inspect consequences of fiber laser processing parameters (scan speed, average power, hatch distance, and frequency) on titanium surface roughness being used as an abutment to enhance shear bond strength (SBS) to resin cement.

**Material and methods:** Forty pure titanium discs have 6 mm x 3 mm (diameter and height respectively) were categorized into four groups (n=10) as following: control group: without any surface treatment, group A: fiber laser application with 3 W average power, pulse duration of 81 ns, 11.9 cm standoff distance, spot size of 0.05 mm, 30 kHz repetition rate, and 10000 mm/sec scanning speed, group B: fiber laser application with 5 W average power, pulse duration of 81 ns, 11.9 cm standoff distance, 0.05 mm spot size, 30 kHz repetition rate, and 10000 mm/sec scanning speed , group C: fiber laser application with 7 W average power, pulse duration of 81 ns, 11.9 cm standoff distance, spot size of 0.05 mm, 30 kHz repetition rate, and 10000 mm/sec scanning speed. Pilot study performed to assess the suitable laser parameters. Characterization of titanium discs done use optical microscope, surface roughness tester and scanning electron microscope (SEM). Phase analyzing was carried out using X-ray diffraction (XRD). Following these

tests, application of resin cement to titanium discs was performed according to manufacturer's instructions. Measuring of shear bond strength (SBS) values were conducted by a universal testing machine. After deboning, surfaces of titanium discs were examined by stereomicroscope for determination of failure modes. Data analysis were performed using SPSS/24 that used ANOVA, Shapiro Wilk and Tukey post hoc (HSD) tests ( $\alpha = 0.05$ ).

**Results:** Positive changes in surface morphology of all experimental groups were noticed. The values of the surface roughness of the irradiated samples by fiber laser are the highest in group (C) followed by group (B) and (A) compared to the control group. Lowest value of shear bond strength (SBS) was with the control group and highest SBS value was occurred with group (C) followed by group (B) and eventually with group (A). Additionally, there is improvement in failure modes in all experimental groups. There was no change in the phase of titanium following laser treatment.

**Conclusion:** The present study revealed that the fiber laser treatment of titanium surface with 30 kHz frequency, 81 ns pulse duration, 0.05 mm spot size, 10000 mm/sec scanning speed, 11.9 cm standoff distance and average power of 7, 5 and 3 W result in a highly significant increase of shear bond strength with resin cement.

## List of contents

<b>Title</b>	<b>Page no.</b>
<b>Chapter one</b>	
1.1 Introduction	1
1.2 Dental implant	2
1.3 Implant abutment	3
1.4 Implant abutment materials	5
1.4.1 Titanium abutment	5
1.4.2 Zirconia abutment	8
1.4.3 Cast gold abutment	9
1.4.4 Surgical grade stainless steel abutment	9
1.4.5 PEEK abutment	10
1.5 Types of abutment - prosthesis retention	10
1.6 Cement-retained vs screw -retained implant prosthesis	11
1.7 Factors that affecting the retention of cement retained implant supported prosthesis	13
1.8 Resin cements	14
1.9 Surface modification of titanium abutment	15
1.0 Methods of titanium abutment surface modification	15
1.10.1 Mechanical methods	15
1.10.2 Chemical methods	17
1.10.3 Combination methods	18
1.10.4 Laser modification technique	19
1.11 Laser basics	20
1.12 Laser material interaction	20
1.13 Advantages of laser	25
1.14 Laser parameters affecting material surface treatment	25
1.15 Fiber laser	29
1.16 Q-switched fiber laser	31
1.17 Laser safety	31
1.18 Literature review	33
1.19 Aims of the Study	35
<b>Chapter two</b>	
2.1 List of Materials and equipment	36
2.2 Methods	37
2.2.1 Titanium discs preparation	37
2.2.2 Laser system	38
2.2.3 Surface roughness measurements	39
2.2.4 phase analysis	40
2.2.5 The pilot study	41
2.2.5.1 First pilot study group	41
2.2.5.2 Second pilot study group (hatch spacing variations)	41

2.2.5.3 Third pilot study group (Scan speed variations)	42
2.2.5.4 Fourth Pilot Study Group (Frequency variations)	42
2.2.5.5 Fifth pilot study group (Average Power variations)	43
2.2.6 Study group	44
2.2.7 The experimental work	44
2.2.7.1 Rubber mold construction	44
2.2.7.2 Cementation procedure	45
2.2.8 Shear bond strength test	48
2.2.9 Modes of failure	49
2.2.10 Statistical analysis	50
<b>Chapter three</b>	
3.1 Results	52
3.1.1 Surface morphology	52
3.1.2 Surface roughness results	61
3.1.2.1 Surface roughness results of the pilot study	61
3.1.2.2 Surface roughness results of control and study groups	63
3.1.3 Analysis of phase	65
3.1.4 Shear bond strength	68
3.1.4.1 Shear bond strength of pilot study group	68
3.1.4.2 Shear bond strength of the study group	68
3.1.5 Modes of failure	71
3.2 Discussion	74
3.2.1 Surface morphology	75
3.2.2 Surface roughness (Ra)	75
3.2.3 Analysis of phase	77
3.2.4 Shear bong strength	78
3.2.5 Modes of failure	79
3.3 Conclusion	80
3.4 Suggestion for future studies	81
References	82

### List of tables

<b>Table Title</b>	<b>Page no.</b>
<b>Chapter one</b>	
Table1.1: A summary of laser classes, possible hazards and safety measures	32
Table1.2: Literature Review	33
<b>Chapter two</b>	
Table 2.1: List of the materials	36
Table 2.2: List of equipment	37



<b>Chapter Three</b>	
Table 3.1: Ra for the group of hatch distance	61
Table 3.2: Ra for scan speed group	61
Table 3.3: Ra for frequency group	62
Table 3.4: Ra for the group of average power	62
Table 3.5: Descriptive statistic of the surface roughness for the study groups	64
Table 3.6: Shapiro-Wilk Test of the study Groups.	64
Table 3.7: ANOVA Test of the surface roughness Data.	64
Table 3.8: Tukey Test between the study groups	65
Table 3.9: Mean SBS of the pilot study groups	68
Table 3.10: Descriptive statistic of SBS for the study groups	69
Table 3.11: Shapiro-Wilk Test of the study Groups	70
Table 3.12: ANOVA Test of the shear bond strength Data	70
Table 3.13: Tukey Test between the study groups	71
Table 3.14: Final results of the experimental groups.	71
Table 3.15: Modes of failure for the study groups.	72

## List of figures

Figure title	Page no.
<b>Chapter one</b>	
Figure 1.1: (a) Parts of dental implant (20) ,(b) Parts of dental implant vs parts of natural tooth.	3
Figure 1.2: Parts of implant abutment in different designs.	4
Figure 1.3: Gold and silver color titanium abutments.	6
Figure 1.4: Crystalline structure of titanium.	7
Figure 1.5: Zirconia abutment.	8
Figure 1.6: Cast gold abutment.	9
Figure 1.7: PEEK temporary abutment.	10
Figure 1.8: (a) Cement retained implant prosthesis, (b) Screw retained implant- prosthesis.	12
Figure 1.9: Absorption spectrum of titanium.	19
Figure1.10: Laser- material interaction phenomena.	21
Figure 1.11: Physical effects of laser-material interaction.	23
Figure 1.12: (a) plasma coupling effect (b) plasma shielding effect.	24
Figure1.13: Effect of long laser pulses versus short laser pulses.	27
Figure1.14: Depth of focus.	29
Figure 1.15: Optical fiber of fiber laser.	30

<b>Chapter two</b>	
Figure 2.1: Titanium discs	38
Figure 2.2: Ultrasonic cleaner	38
Figure 2.3: Fiber laser	39
Figure 2.4: Surface roughness tester.	40
Figure 2.5: X-ray diffraction machine.	40
Figure 2.6: (A) Control specimen without laser treatment and (B)-(E) specimens irradiated at a standoff distance of 119,120,121 and 122 mm respectively.	41
Figure 2.7: (A) Silicone rubber mold (B) cross section of the molded test specimen.	45
Figure 2.8: Acrylic blocks of titanium discs.	46
Figure 2.9: Positioning of the silicone mold.	46
Figure 2.10: Breeze self-adhesive resin cement.	47
Figure 2.11: Cementation procedure over the titanium disc.	47
Figure 2.12: Light curing device	48
Figure 2.13: Water bath	48
Figure 2.14: Universal testing machine	49
Figure 2.15: Chisel-end blade	49
Figure 2.16: Stereomicroscope	50
<b>Chapter three</b>	
Figure 3.1: Optical microscope images of titanium discs with different hatch distance.	53
Figure 3.2: Surface morphology of the control specimen	54
Figure 3.3: surface morphology of 3 W group	55
Figure 3.4: Surface morphology of 5 W group	56
Figure 3.5: Surface morphology of 7 W group	57
Figure 3.6: Surface morphology of 10 W group	58
Figure 3.7: Surface morphology of 30 W group	59
Figure 3.8: Surface morphology of 50 W group	60
Figure 3.9: Ra for titanium discs as function of laser parameter	63
Figure 3.10: XRD pattern of control and (3 W, 5 W, and 7W) laser irradiated specimens.	66
Figure 3.11: XRD pattern of control and (10 W, 30 W, and 50W) laser irradiated specimens	67
Figure 3.12: Bar chart of SBS mean of the study groups.	69
Figure 3.13: Distribution of failure mode in the study groups.	72
Figure 3.14: Stereomicroscope images of modes of failure.	73

## List of abbreviation

Symbol	Term
AFM	Atomic force microscope
ANOVA	Analysis of Variance
Al <sub>2</sub> O <sub>3</sub>	Aluminium Oxide
CAD CAM	Computer aided design and computer aided manufacturing
cm <sup>2</sup>	Square centimeter
CO <sub>2</sub>	Carbon dioxide
CP Ti	Commercially pure titanium
E	Energy
EDM	Electro Discharge Machining
EDS	Energy dispersive spectroscopy
Er,Cr:YSGG	Erbium, chromium: yttrium-scandium-gallium-garnet
Er:YAG	Erbium: yttrium-aluminum-garnet
E.T	Exposure time
F	Frequency
Hz	Hertz
ICDD	International Centre for Diffraction Data
J	Joule
kHz	Kilohertz
Kv	Kilo voltage
kW	Kilo watt
mA	Milliampere
mJ	Millijoule
µm	Micrometer
MOF	Modes of failure
MPa	Mega pascal
Nd:YAG	Neodymium-doped yttrium aluminum garnet
Nm	Nanometer
OPT	Oxygen plasma treatment
P	Power
P <sub>p</sub>	Peak power
P average	Average power
PEEK	Polyether ether ketone
Ra	Average surface roughness
S	Second
SBS	Shear bond strength
SD	Standard Deviation

SEM	Scanning Electron Microscope
SPSS	Statistical package for the social sciences
Ti	Titanium
TiN	titanium nitride
TiO <sub>2</sub>	Titanium dioxide
Ti-6Al-4V	Titanium -6 Aluminium-4Vanadium
Tp	Pulse duration
Tukey's HSD	Tukey's Honestly Significant Difference
W	Watt
wt.	Weight
XRD	X-ray diffraction
Yb	Ytterbium
$\lambda$	Wavelength

# **CHAPTER ONE**

## **INTRODUCTION AND BASIC CONCEPTS**

# CHAPTER ONE

## 1.1 Introduction

Dental implants have successfully added to the restorative options to treat both partially and completely edentate patients in the world of dentistry. As a result, their masticatory function and aesthetics are restored (1). Over the last few decades, advancement in the design and engineering of dental implants have progressed. These advancement had resulted in a success rate of more than 90 % and a survival rate of more than ten years (2-4).

As dental implants become more widely used in practices around the world, the question then becomes how to improve delivery and maintenance of dental-implant treatment.

In general, dental implant consist of three parts: implant fixture, implant abutment, and prosthetic crown. Implant treatment success is significantly affected by implant abutments; they may have an enormous effect on the esthetic, functional aspects, and long-term prognosis of implant treatment (5). Different materials had been used in construction of implant abutments and the most commonly used materials are titanium (1, 6, 7). Titanium with its exceptional properties and superior biocompatibility made a noticeable entry in dentistry; it is a material with low density, highly resistant to corrosion, suitable strength to weight ratio, and excellent thermal conductivity (8) .

The connection of the crown or the final restoration to the implant abutment can be via either screw or cement (9). The security of retention between implant abutment and crown is the main factor that contributes to success of cemented restoration (10). One of essential factors that affect bonding of cemented restoration is area of the surface (11).

Retention of the cemented restorations is enhanced by roughness of surface due to increased surface area through creation of micro retentive grooves and

ridges (12). Various techniques were used to enhance the bonding characteristics by surface modification of titanium abutment such as sandblasting, acid etching, electro discharge machining, grinding with bur, or a combination of these methods. Studies have shown that these techniques affect the bond strength at various amount (7, 13, 14).

With advancement in technology, laser have been used as alternative method for titanium surface modification because they are highly efficient and easily used. Laser treatment was suggested by many authors as a substitutional method of surface treatment for increasing the surface roughness of titanium abutments and enhance their retention using different wavelength such as Nd:YAG laser (9, 15, 16), Er:YAG laser (9), Er,Cr:YSGG laser (10), CO<sub>2</sub> laser (17) and ultrafast fiber laser 1064 nm (14). According to the author's knowledge, Studies that investigate the impact of fiber laser 1064 nm on the adhesion efficiency between titanium and resin cement are very limited. Accordingly, the objectives of the present study is to evaluate the impact of fiber laser parameters on surface roughness and bond strength of resin cement to titanium.

## **1.2 Dental implant**

“a prosthetic device made from alloplastic material implanted into the oral tissues beneath the mucosa and/or periosteal layer, and on/ or within the bone, to provide retention and support for fixed or removal dental prosthesis " (18).

In general, dental implant consist of three parts as shown in (figure 1.1) (19):

1. Implant fixture: is the part that simulates the root of natural tooth.
2. Implant abutment: the part that connect the prosthetic crown to the implant.
3. Crown: the prosthetic part that substitutes the natural tooth.

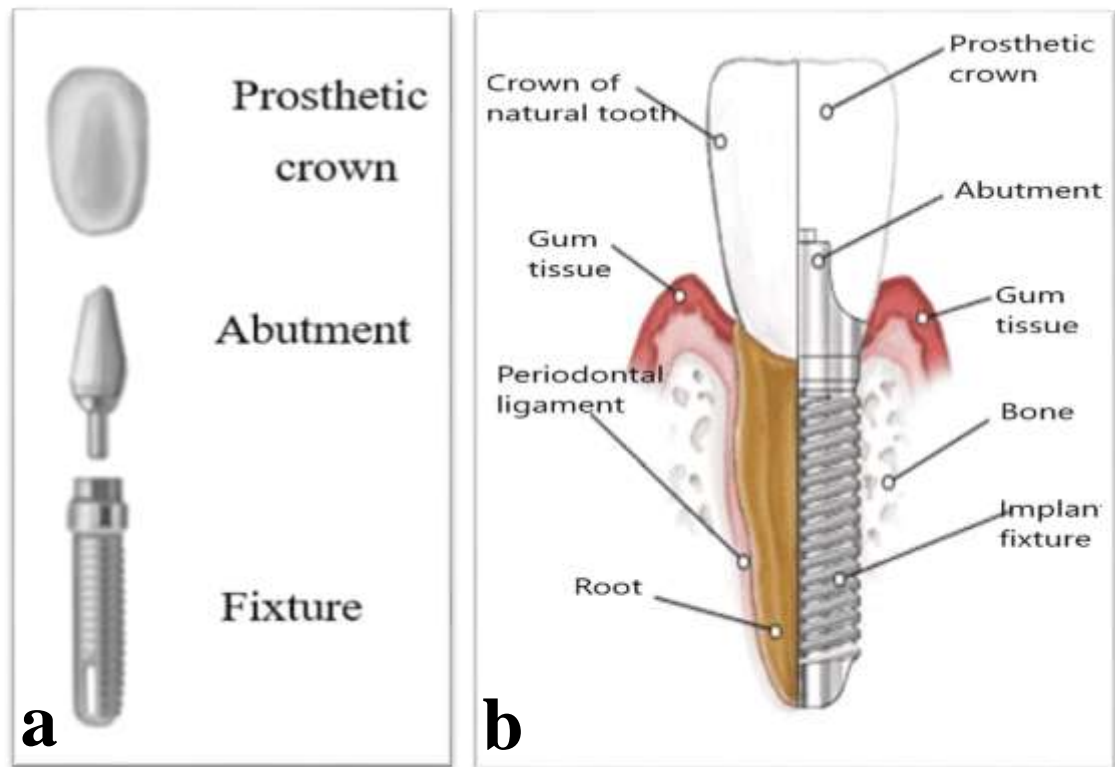


Figure 1.1: (a) Parts of dental implant (20) ,(b) Parts of dental implant vs parts of natural tooth (19).

### 1.3 Implant abutment

The definition of implant abutment according to Glossary of dental implantology 2018 was “The component that interfaces with the implant fixture (implant body) and the prosthetic entity” (21).

Implant abutment can sub-divided into two types according to the method of fabrication:

1. Prefabricated abutment: that fabricated by the same company that manufactured the implant.
2. Customized abutment: that fabricated with CAD/CAM or as a customized cast (1).

Moreover, abutments available either as a separated segment or become incorporated with the prosthetic part or with the implant (22).



Generally, abutment divided into three parts as shown in (figure 1.2):

1. Implant connection part: is the inferior part of the abutment, which connected with the implant.
2. Prosthesis connection part: is the Superior part of the abutment, which connected to the prosthesis.
3. Transgingival part: the part of the abutment, which surrounded by the gingiva directly above the implant platform (5).

The inferior part of the abutment is the only part that must not be changed while the other parts modified to enhance the implant treatment results.

The modification of the prosthesis connection part based on several factors such as the shape, size, and prosthesis emergence profile, the interocclusal space, and material type of the prosthesis that determine the amount of clearance for example gold crown needed less reduction while ceramic and porcelain fused to metal crown (PFM) needed more reduction (23).



Figure 1.2: Parts of implant abutment in different designs (23).

## 1.4 Implant abutment materials

Various materials used for fabrication of abutments include:

1. Titanium.
2. Zirconia
3. Cast gold.
4. Surgical grade stainless steel.
5. Polyether ether ketone (PEEK) (23).

### 1.4.1 Titanium abutment

In the field of dental implantology titanium is widely used either as a pure or in the form of alloy (24). Alloying of titanium is usually done with metals for example Aluminum (Al) and Vanadium (V), for modification of its physical properties (25).

Titanium is highly reactive metal, when it exposed to air, immediately it form passive layer of titanium oxide on the surface. Therefore, Titanium has high corrosion resistance and excellent biocompatibility (7). Titanium has low density ( $4.51 \text{ g/cm}^3$ ), high melting point ( $1668^\circ \text{ C}$ ), elastic modulus (117 GPa) and low coefficient of thermal expansion ( $9.4 \times 10^{-6}/^\circ \text{ C}$ ) (26). Also titanium has satisfactory strength to weight ratio, because of these physical properties titanium displays significant advantage in the field of dental implantology (27, 28).

Implant abutments made either from titanium alloy or from commercially pure titanium (5, 23).

Titanium abutments are the primary option for posterior implants because of titanium excellent physical properties. These abutments are available as CAD/CAM milled customized or prefabricated stock abutment.

They are either silver or gold in color; the gold color of the titanium abutment is due to titanium nitride (TiN). This type of abutment most commonly used in esthetic zones. TiN coating improve surface properties of the substrates and give an esthetic imitation with the overlying gingival tissue. The thickness of TiN coating is less than 5  $\mu\text{m}$  therefore it is suitable only for abutment milled with CAD/CAM technique because in prefabricated type a minimal adjustment will destroy the coating **(23)**.

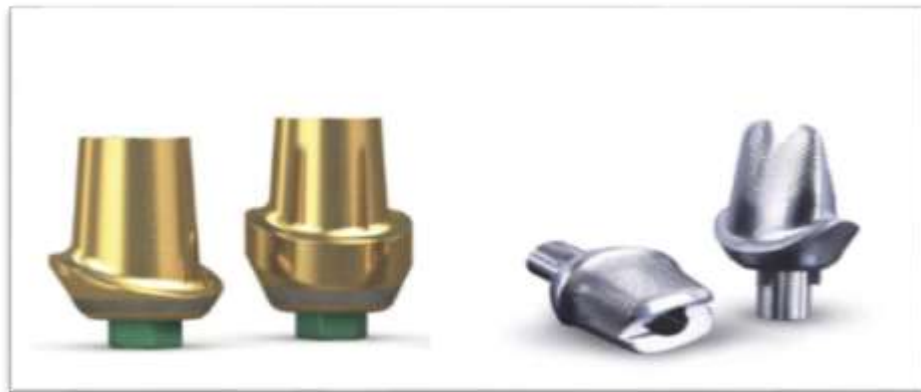


Figure 1.3: Gold and silver color titanium abutment **(23)**.

Pure titanium consist of 99.5% titanium and 0.5 of elements such as (oxygen, nitrogen, carbon, iron and hydrogen) **(29)**.

There are four grades of commercially pure titanium (CP Ti) based on purity and oxygen content (0.18 to 0.40 wt. %) which are (CP Ti grade 1, CP Ti grade 2, CP Ti grade 3 and CP Ti grade 4)

These small differences have a significant impact on mechanical and physical properties of commercially pure titanium, they differ in strength, corrosion resistance and ductility, CP Ti grade 4 as a result of its highest oxygen Content (about 0.4 wt.%) has the maximum mechanical strength among the other grades **(30, 31)**.

Pure titanium is considered an allotropic element and at 882°C its crystalline structure undergo transformation from hexagonal closed pack crystal (alpha

phase) to body centered cubic crystal (beta phase) (figure 1.4) until melting of titanium at 1668 °C (32).

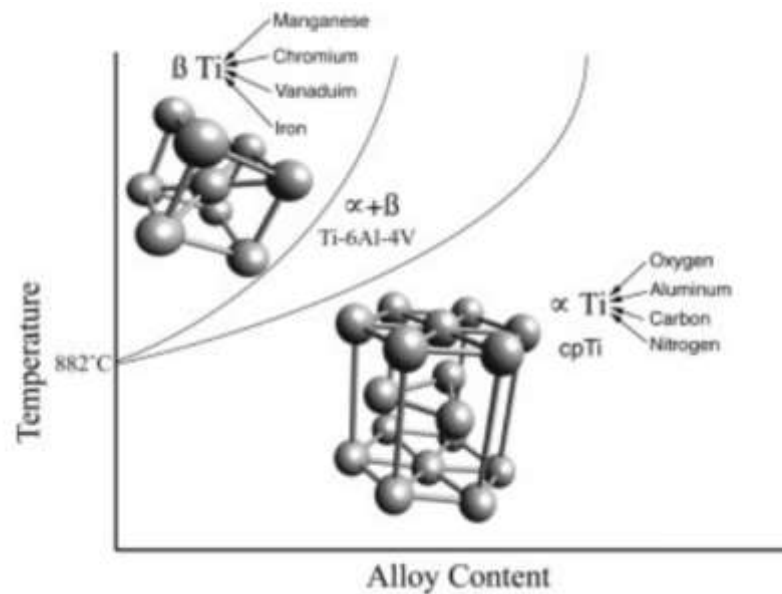


Figure 1.4: Crystalline structure of titanium (33).

Grade 5 titanium is another name of titanium alloy (Ti-6Al-4V), its consist of 6% aluminum, 4% vanadium , 0.2% oxygen (maximum) , 0.25% iron - (maximum) and the remainder titanium (34). It is stronger than commercially pure titanium and provide superior fracture resistance and tensile strength (23).

Titanium alloy classified as either  $\alpha$ -type or  $\alpha+\beta$ -type or  $\beta$ -type alloy, depending on the type and quantities of alloying elements (35). Ti-6Al-4V alloy ( $\alpha+\beta$ -type) alloy is the most widely used for medical application.

Ti-6Al-4V alloy is biocompatible has good resistance to corrosion, high strength, and good weldability (25).

Incorporation of aluminum and vanadium into titanium alloy will increase the material hardness, therefore it has better mechanical, physical properties and more resistance to fatigue than CP Ti (29).

Although grade 5 titanium is stronger than CP Ti, its slow releasing of aluminum and vanadium may lead to health hazards because aluminum cause neurological disorders and vanadium is highly toxic both in its oxide and in state forms (26).

### 1.4.2 Zirconia abutment

Implant abutment can also fabricated from zirconia (figure 1.5), because zirconia offered favorable optical characteristics, good biocompatibility, lower corrosion, lower thermal conductivity, and lower plaque accumulation (36, 37)

However, Because of the reduction in the mechanical strength, zirconium abutments had more mechanical complication than titanium abutments, this is the key drawback for the limited application of zirconium abutments (38, 39). Zirconia abutment is suitable to use in anterior area because of its mechanical properties but there is no adequate evidence of using zirconia as a posterior implant abutment (40). In vitro studies concluded that titanium abutment is better than zirconia abutment both in fatigue reliability and in fracture resistance (41, 42). Zirconia abutments mostly fractured at their apical portion, which it is the thinnest region (22).



Figure 1.5: Zirconia abutment (43).

### 1.4.3 Cast gold abument

Cast gold abument consist of a pre-machined gold base which fit to the corresponding implant head and a plastic cylinder that can be cut, modified and waxed prior to alloy casting (44).

This type of abutment are used for fabrication of implant-level, height reduction to obtain occlusal clearance vertically and/or custom angle and for provding esthetically sub-gingival margins (45). However, cast gold abutment has some disadvantages that its costly and its fabrication is complicated in which investing , casting and polishing could be susceptible to manufacturing inaccuracy (46).



Figure 1.6: Cast gold abutment (47).

### 1.4.4 Surgical grade stainless steel abutment

Surgical grade stainless steel abutment is mainly used as temporary abutment. It is consist of stainless steel alloyed with elements such as nickel, chromium, and molybdenum. Nickel gives smooth, polished surface while chromium increase the corrosion resistance and molybdenum incease material hardness.

This type of abutment is strong, high resistant to corrosion, easily sterilized and cleaned but its nickel content may lead to immune complication (23).

### 1.4.5 PEEK abutment

Polyetheretherketone (PEEK) is a synthetic polymer, which has good biomechanical strength, and inactive chemical properties, this made it favorable to use in medical purposes.

PEEK abutments are used as a temporary abutments for implant supported provisional crown (**1, 48**) and it is used in esthetic zones in cases for not more than three months under load (**49**).

PEEK abutment has a significant vertical displacement compared to titanium abutment, as well as deformation of plastic at implant-abutment interface, all of which can result in high torque loss and micro leakage of PEEK abutment that made it not suitable to be an alternative to titanium abutment (**50**).

Although carbon fiber reinforcement of PEEK abutment (CFR/PEEK) improves biomechanics, there are some drawbacks to this process, such as black color and tissue inflammation when the fiber dislodge from PEEK core (**51**).



Figure 1.7: PEEK temporary abutment (**52**).

## 1.5 Types of abutment - prosthesis retention

According to the technique by which the Implant-supported prosthesis attached to the implant, they divided into two types:

1. Cement retained implant restoration.
2. Screw retained implant restoration.

Cement retained type restoration retained onto the abutment by using cementing medium, whereas in screw retained type the restoration directly attached to the implant or to the abutment **(53)**.

Clinical standards for example esthetic, ease of fabrication, prosthesis maintenance and retrievability, occlusion, and cost may affect the decision of which retention mechanism is used **(54)**.

## **1.6 Cement-retained vs screw -retained implant prosthesis**

In spite of the fact that, there is no agreement on which method of retention is the best, cementation of implant supported prosthesis is preferred by many clinicians more than screw fixation **(14, 55)**. Technically and clinically the procedure of cement retained type is similar to that used for reconstruction of tooth born, therefore it is easier to be fabricated and manipulated intraorally **(56)**.

Furthermore, the rate of complication is lower and the fracture resistance of ceramic veneer is higher **(57, 58)**.

Cement-retained type also have the advantages of better esthetic and intact occlusion due to absence of occlusal opening (that present in the screw retained type) as shown in (figure 1.8), the ability to compensate of the improperly inclined implant , lower cost and the passive adjustment is easier than screw retained type **(59, 60)**.

The main disadvantages of cement-retained type that its removal is difficult than the screw type, and the removal of excess cement from sub gingival area is difficult **(49)**.



While the screw-retained type has an advantage of ease of retrieval especially in cases when the retaining screw become loose or when the veneering chipped.

In cases of limited interocclusal distance screw retained type is more indicated than cement retained type (61), because the retention of cement retained restoration affected by surface area and height, therefore in cases that the interocclusal distance is less than 4 mm screw retained type is indicated (1, 62), although this can be overcome by surface modification of the abutment to increase surface area which improves retention (17).

However, at the screw-hole interface of the screw retained type there is lower porcelain strength (63) also Torrado et al. concluded that lower force needed to induce fracture in screw-retained types in comparison with the cement-retained types (61).

Moreover, the screw is smallest and weakest component that link the implant parts and it is susceptible to fracture or loose before the other components failure (64). As a result of function loading as mastication, the incidence of screw loosening is high (5, 65).

Fracture of screw as a result of applying excessive torque during insertion is another complication of screw retained type (66).

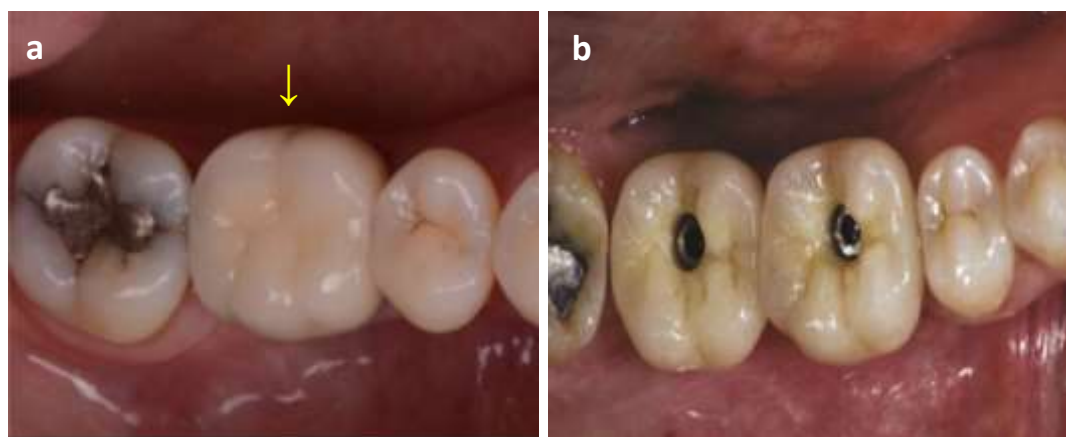


Figure 1.8: (a) Cement retained implant prosthesis (67), (b) Screw retained implant-prosthesis (68).

## **1.7 Factors that affecting the retention of cement retained implant supported prosthesis**

One of principal factor affecting longevity of the implant supported prosthesis is the security of retention and this performed by enhancing the bonding between implant abutment and cement **(10, 16)**.

The retention of cement retained restoration is affected by many factors for example height of abutment and surface area, abutment taper, luting cement and finish or roughness of surface **(69)** .

Abutment height is directly proportionate with the retention. As the height of abutment increase, the surface area increased, therefore the retention of cement remarkably increased **(70-72)**.

However abutment height and configuration are factors that determined by the clinical status and cannot be altered according to the choice of the clinician **(69)**.

The ideal taper for tooth preparation is  $6^\circ$  taper **(17)**, therefore most of the manufacturers machine the abutment with  $6^\circ$  taper. Furthermore, abutments with  $6^\circ$  taper provide better bond strength when compared with angled abutment **(73)**.

The most important factors that can be controlled by the clinician for increasing retention are the surface roughness and the type of luting cement **(69)**.

Studies by Cano-Batalla et al., Usten et al., and Veljee et al. demonstrated that surface modification of abutment lead to increase the bonding area and in turn, the retention improved **(10, 28, 71)**.

Retention of restorations increase by roughness of surface owing to formation of microretentive ridges and groove pattern and in turn the surface area increased **(12, 74)**.

Cementation of the prosthesis to the abutment can be performed either by provisional cement or by definitive cement. The retention value of provisional cements are smaller than that of the definitive cements (60), therefore provisional cement used for cases in which retrievability is required (69).

## 1.8 Resin cements

Resin cements are the modern type of cement for indirect restorations, and they have the potential to bond between the abutment and the restoration's internal surface. They are composed of the same basic ingredients as composite restorative materials, but with less filler particles (75). These cements have higher compressive, flexural, and tensile strength and wear resistance than the conventional cements and can be used for any restoration type and with any restoration material. They come in different shades and are virtually insoluble in oral fluids providing better marginal seal than any other cement types.

Resin cement can be classified according to their adhesive characteristics into three types include: etch-and-rinse resin cements, also called total-etch cements, the self-etch resin cements, and the self-adhesive resin cements.

Etch-and-rinse cements and self-etch cements types require adhesive pretreatment of the abutment surface, i.e., etching, priming, and bonding. While self-adhesive resin cements they can bond to abutment surface without the need for prior etching and bonding (76).

Resin cements can also be classified according to modes of polymerization into:

1. Self-curing resin cements which set through chemical reaction and are especially useful in areas that are difficult to reach with light.

2. Light-cured resin cements which set exclusively through light polymerization.

3. Dual-cured resin cements which are cured by both light and chemical curing, these types of cements contain self-cured initiator and light-cured initiator (77). The initial setting of cement is achieved with light curing to seal the gingival margins quickly (78). The self curing components ensures that the cement will be cured underneath restoration that is too thick or too opaque to allow light transmission of through it (79). Although dual cured resin cements can be set through chemical reaction alone, they still require light curing to achieve a high degree of polymerization (76).

## **1.9 Surface modification of titanium abutment**

The retentive strength of cemented prosthesis could be improved by modification of surface characteristic and roughness of implant abutment in comparison to the surface of uniform implant abutment (12).

There are many methods for surface treatment of titanium abutment and this methods include surface roughening to obtain micromechanical retention, chemical bonding between titanium surface and luting cement, or combination methods that combine both chemical and micromechanical methods (80).

## **1.10 Methods of titanium surface modification**

It include the following methods:

### **1.10.1 Mechanical methods**

**a. Oxygen plasma treatment (OPT):** It is a non-invasive procedure which involve forming an oxide layer on titanium surface without producing micro retentive areas (81).

Non-thermal plasma (NTP) is done at different atmospheric pressure by application of various gases for example oxygen plasma and using homogenous dielectric barrier discharge for certain period of time **(82)**.

Tseng et al., 2013 demonstrated that the longer application of OPT for more than 5 min lead to decrease in surface roughness because this will lead to reverse the effect of oxygen plasma treatment. After the formation of titanium oxide layer ,the rate of titanium oxidation become stable and the effect of oxygen plasma will only induce smoothing of the surface **(83)**.

Non-thermal plasma treatment only induce change in the chemistry of the surface and has no cytotoxic effect **(84)**.However, it is not effective method for roughening titanium surface comparing with other micromechanical methods **(82)**.

### **b. Sandblasting technique:**

This technique involve using a stream of high-speed  $\text{Al}_2\text{O}_3$  particles pushed by pressed air, it increase the surface roughness by increasing the area of bonding surface **(85)**.

This method which is the most commonly used method to create micro retentive areas for receiving resin cement or bonding resin **(8)**.

As a result of increasing metal surface area by sandblasting technique, the mechanical interlocking between the cement and abutment surface increased and this result in higher retentive cement **(69)**. However, sandblasting method is sensitive technique **(86)**.

The significant disadvantages of this method are contamination and metal substrate distortion by air born particle **(87, 88)**. Also the bonding strength may be compromised by impurities that produced by sandblasting method **(7)**.

### c. Grinding with diamond bur

Using of diamond bur is another method for Surface modification of titanium abutment by grinding titanium abutment with diamond rotary-cutting instrument on high speed handpiece. However, this method was not effective as sandblasting or laser modification methods for improving retention (14, 74).

## 1.10.2 Chemical method

a. **Chemical etching:** Chemical etching is a substitute procedure to sandblasting for increasing retention of titanium abutment to the prosthetic part (89).

It is performed by submerging the titanium into different concentration of inorganic acids for certain period of time such as hydrochloric acid HCl (13), hydrofluoric acid (HF) and nitric acid (HNO<sub>3</sub>) (15, 90) or as a mixing of inorganic acid such as of phosphoric acid (H<sub>3</sub>PO<sub>4</sub>), sulfuric acid (H<sub>2</sub>SO<sub>4</sub>), hydrofluoric acid (HF) and hydrochloric acid (HCl) (16).

However, Kim and Cho reported that laser modification of titanium improving the bond strength more than acid etching method (13).

b. **Chemical bonding:** by using silanes and metal primer (91). The resin matrix of silanes bonded chemically with the surface of metal (92).

While Metal primers have active monomers for example methacryloyloxyalkyl thiophosphate derivative (MEPS), 10-methacryloyloxydecyl dihydrogen phosphate (MDP) and 4-methacryloyloxyethyl trimellitate anhydride (4-META) that chemically react with the metal surface oxides (93). The adhesive effect of metal primer can

vary because metal primer different types have various active monomers (94).

### **1.10.3 Combination methods**

#### **a. Coating with tribochemical silica**

This system involve a combination of both chemical and micromechanical adhesion (93).

It consist of two steps:

First step is air abrasion with 30 or 110  $\mu\text{m}$  silica-modified  $\text{Al}_2\text{O}_3$  particles and the second step is the application of silane (6, 93, 95).

#### **b. Electro Discharge Machining (EDM)**

EDM also known as spark erosion. It is a thermoelectric technique that is used to change material surface in dentistry, in which the work piece is immersed in dielectric fluid which representing the cathode of an electrochemical cell and the Cu implant analogues representing the anode (96).

After charging the electrochemical cell, removing of material from abutment done by melting and evaporation in single sparks (14).

This induce changes in morphology and composition of abutment surface that treated with EDM, which exhibit roughening in texture and formation of pores and craters. These surfaces have a recast layer of a few microns in thickness resulted from dielectric fluid and electrodes decomposition (96).

### 1.10.4 Laser modification technique

Because of development in dental technology, lasers more commonly used in dental practices and in surface modification of dental materials. Studies have revealed that applications of laser for example Nd: YAG laser, CO<sub>2</sub> laser, Er,Cr:YSGG laser to modify titanium and titanium alloy surfaces leading to improve the bonding strength (10, 17, 97), in addition to fiber laser that have been effectively used in dentistry for surface modification of titanium and to improve the bonding strength (14, 98, 99).

Several studies demonstrated that laser could be used for surface modification of microstructure of titanium surface providing improvement in roughness without contamination (100-102).

The absorptivity spectrum of titanium is in the infrared spectral region (IR). The highest absorption is in near IR region followed by mid IR then far IR region as shown in (figure 1.9) (103).

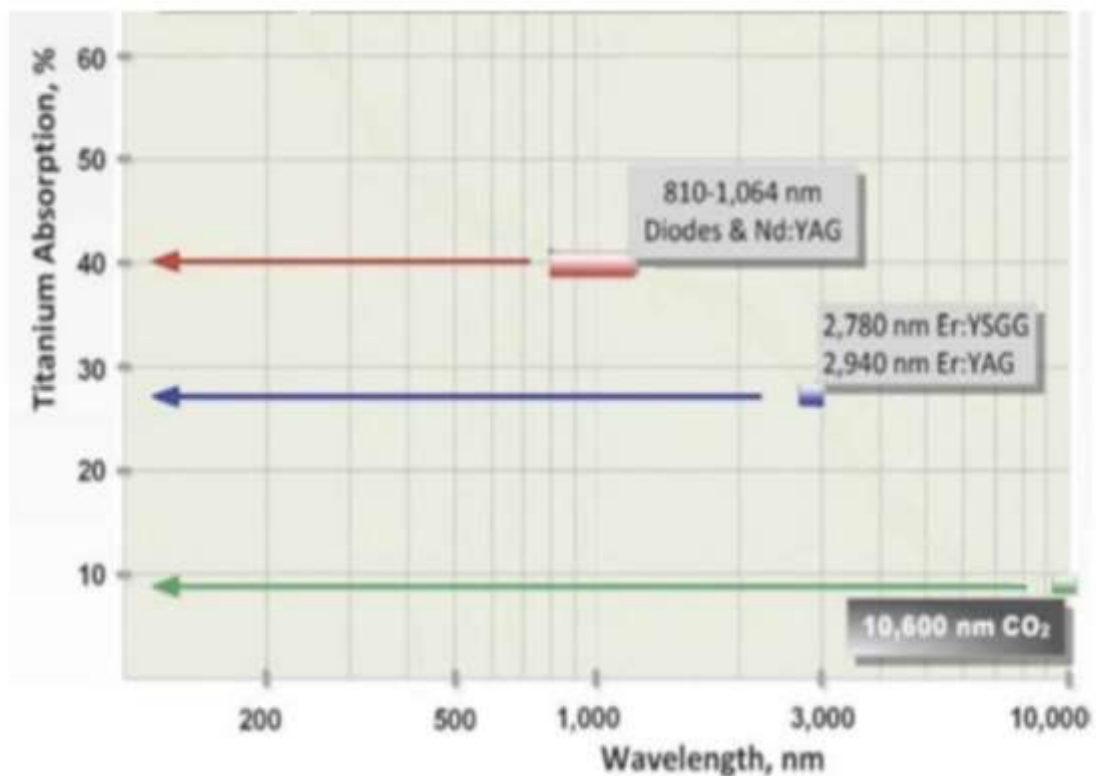


Figure 1.9: Absorption spectrum of titanium (103).



## 1.11 Laser basics

The term of laser is an acronym of "Light Amplification by Stimulated Emission of Radiation".

Lasers wavelength cover a wide portion of the electromagnetic spectrum such as UV, visible and IF regions of electromagnetic spectrum **(104)**.

Laser has the following special properties:

1. Coherence: laser device produces waves that are physically identical therefore the laser beams are all in a fixed phase relation to each other. They have similar frequency and identical amplitude **(105)**.
2. Monochromaticity: Ordinary light is a polychromatic in nature (multi wavelengths or multi colors), while lasers beam is monochromic in nature (single wavelength) **(106)**.
3. Collimation: laser beam is collimated (laser waves are travelling parallel to each other for long distance in one direction with minimal divergence). This property allow the laser wave to be focused with very high intensity **(107)**.
4. Brightness: This property is generated from the ability of the laser beam to be focused in small area with high degree of energy consternations .this phenomena is related to the high degree of collimation of the laser beam **(108)**.

## 1.12 Laser material interaction

When laser beam hit the surface of material, part of it will be returning at the matter surface, the another part of the laser beam will be absorbed by the matter or scattered, and transmission of laser beam through the matter may take place when the matter is transparent and the intensity of the applied laser beam is high (figure 1.10) **(109)**.

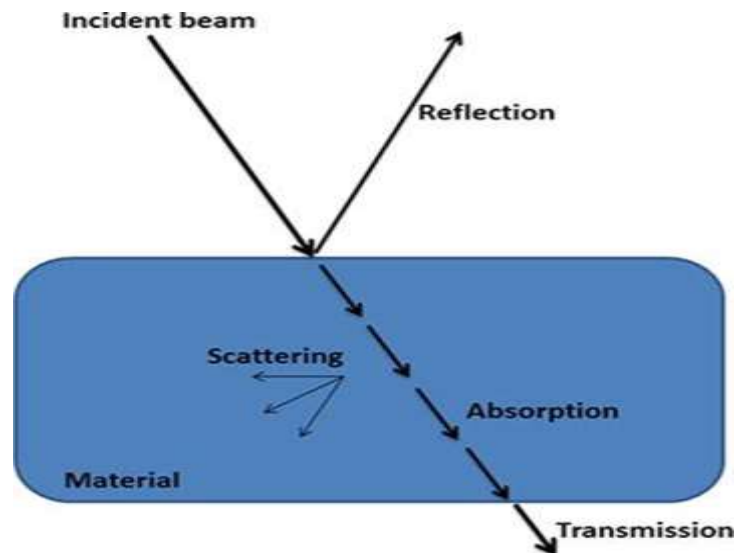


Figure1.10: Laser- material interaction phenomena **(110)**.

The most important and desired phenomenon is absorption in which the interaction between the laser radiation and the electrons of the matter take place.

Laser energy absorption by material depends mainly on the laser wavelength, angle of incidence, spectral absorptivity, and surface roughness of material **(111)**.

During laser material interaction absorbed optical energy of the laser radiation is converted to thermal energy. Furthermore, the interaction of laser with the materials also associated with photochemical process and photoablation.

Following thermal interaction of laser with materials, these physical effect (heating, melting, vaporization, plasma formation and ablation) may take place in the matter depending on the temperature rise magnitude **(112)**.

These physical effects play an important role in laser-materials processing and for each specific effect there is a distinct combination of interaction time and laser intensity.

## 1. Heating

This process happens when the sufficient intensity (about  $10^4$  W/cm<sup>2</sup>) of the incident laser radiation heats the matter without phase transformation as shown in the figure 1.11 (a) **(112)**.

Absorption of the incident laser radiation leads to elevating in the temperature of material but this temperature is below the melting threshold of material **(113)**.

## 2. Melting

At higher intensity of laser radiation, the surface temperature of materials reaches the point of melting and the removal of material by melting occurs figure 1.11 (b).

The pulse duration and the power density of the laser radiation are the governing factors for determining the melting depth **(114)**.

## 3. Vaporization

When the intensity of the incident laser radiation heats the material above its boiling threshold, the material is removed by vaporization. After starting of the vaporization process, the vapor – liquid interface begins and moves further inside the material associated with material removal from above the interface area by evaporation fig 1.11 (c) **(112)**.

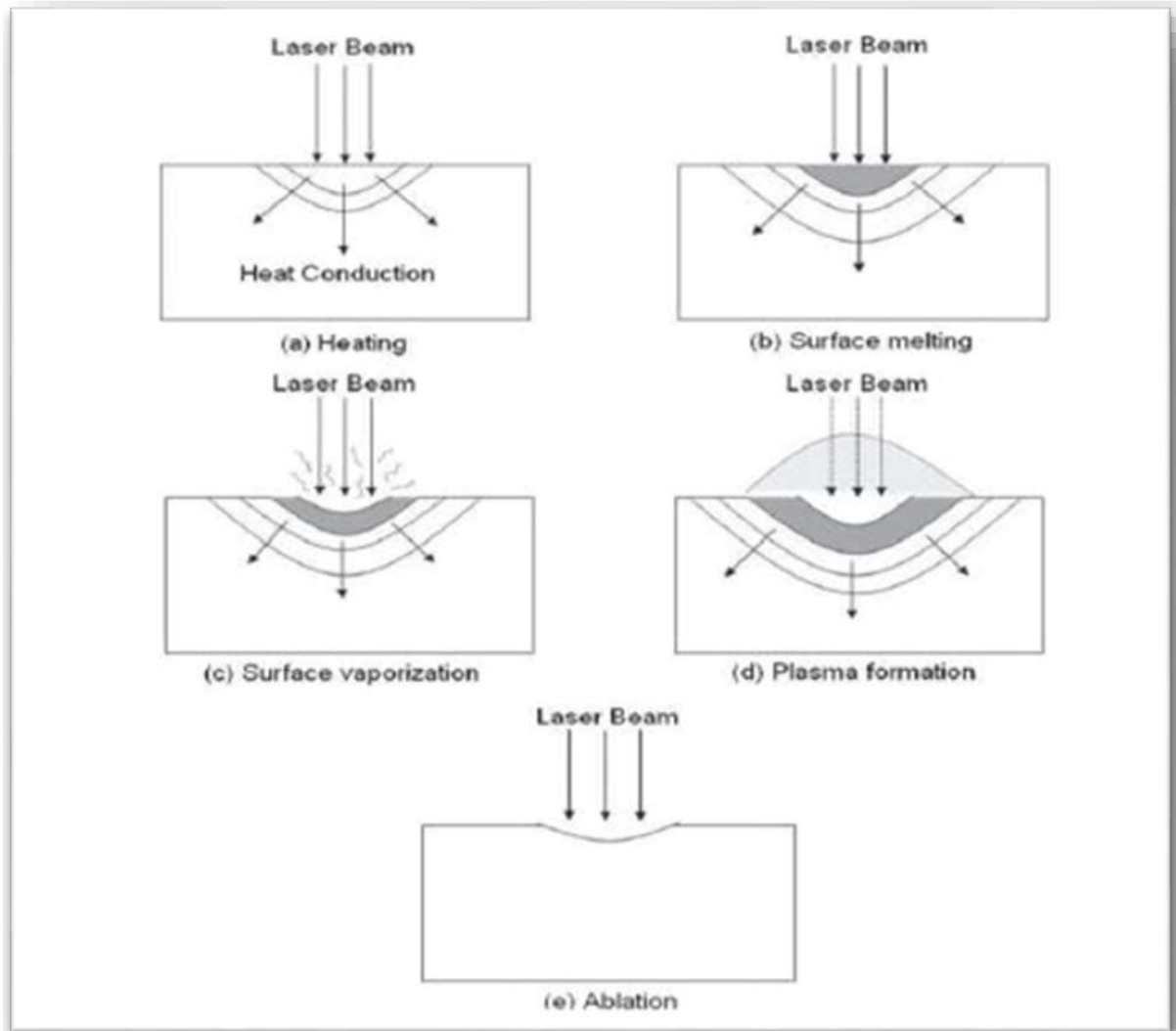


Figure 1.11: Physical effects of laser-material interaction (115).

#### 4. Plasma formation

Plasma formation process take place when the intensity of the incident laser radiation is sufficiently larger to ionize the vapor figure1.11 (d). This vapor, which is highly ionized, is known as plasma.

plasma generation either influence or interfere with interaction between the laser and the materials .When laser intensity sufficient to ionize the vapor ,plasma is formed near evaporating surface of material and it is called

(plasma coupling) which play important role in increasing the absorptivity of laser especially with highly reflective materials .

While as intensity of laser increased significantly, propagations of plasma out of surface of evaporating take place and laser is absorbed inside the plasma and this is called (plasma shielding) as shown in the (figure 1.12) **(112)**.

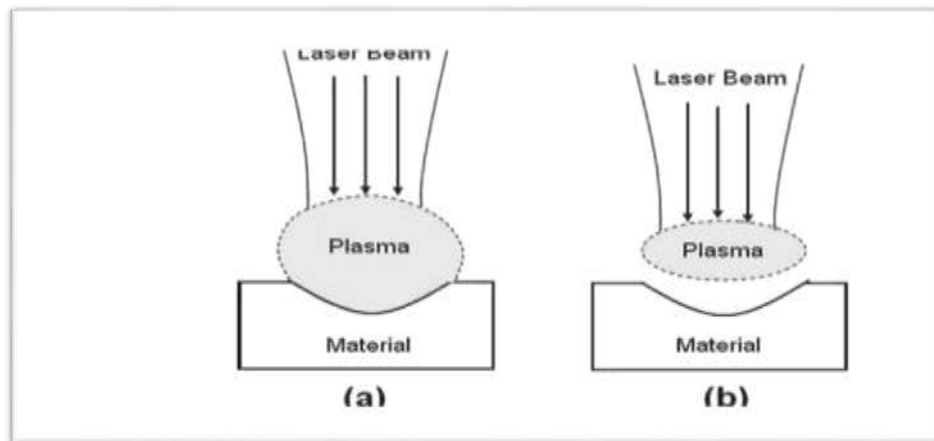


Figure 1.12: (a) plasma coupling effect (b) plasma shielding effect **(112)**.

## 5. Ablation

Ablation is material removal process from the surface of solid as a result of interaction with highly intense short pulses of laser, it occur directly after laser energy absorption by the material without passing through heating or melting processes figure 1.11 (e).

Laser intensity, laser wavelength and pulse duration are the important parameters that affecting the process of ablation **(116)**.

Material removal by ablation process either done by photothermal interaction (as a result of thermal stresses) which take place when energy of laser is below threshold of ablation , or by photochemical interaction (as a result of bond breaking) which take place when energy of laser is above threshold of ablation **(117)**.

## **1.13 Advantages of laser**

The advantages of using laser for surface texturing of the material include **(111, 118, 119)**:

- a) High productivity.
- b) Chemically cleanliness.
- c) Fast speed processing
- d) Minimum Heat affected zone.
- e) By automation adaptability of laser parameters, the thermal affected depth could be controlled.
- f) Non –contact process.
- g) Reduction of cost.
- h) Reduction of the finishing process.

## **1.14 Laser parameters affecting material surface treatment**

To obtain maximum efficiency and best quality in laser treatment process, it is important to run the laser machine at optimal operating parameters. The quality of the surface treatment and the product are dependent on combination of many processing parameters **(120)**.

### **1.14.1 Laser wavelength**

The working wavelength of the laser is the most important parameter to consider during the manufacturing of substances. The absorptivity of matter is significantly depend on the wavelength of the laser. Extreme material absorption of laser wavelength was required in laser-constructed production because the incident laser light must interact properly with the target material **(121)**.

The impact of laser wavelength on laser operating efficiency usually thought of in terms of reflectivity, which varies depending on the incident wavelength and material type. It is obvious that less beam reflectivity means more energy is absorbed **(120)**.

### **1.14.2 Laser power**

The principal factor affecting on depth and width of the laser-affected zone is laser power. If the power of the laser increased, the energy input increases progressively, causing more substrate melt and, as a result, the depth increased after rapid solidification. When the laser power raised, the molten time of the laser-affected zone becomes longer, consequently resulted in increasing the width of the affected zone **(122)**.

### **1.14.3 Pulse duration**

Pulse duration is the period of the laser pulse for each cycle. The Pulse duration is a significant parameter for increasing the pulse energy.

$$E = P_p * t_p$$

Where;

E: laser energy ,  $P_p$ : Peak power,  $t_p$  : Pulse duration.

From the equation, it can be shown that, when the peak power value was constant, the only way to increase the value of the energy was to increase the pulse duration **(123)**.

Longer pulse duration resulted in a pronounced heating effect, increased penetration, resulting in high thermal stresses that inevitably lead to cracking, solidification of the melt ejections that form surface debris, and voids as shown in figure 1.13 (a) **(124)**.

While with shorter pulse duration, peak power can be maximized, while thermal diffusion to the surrounding bulk work material is minimized, resulting in shallow penetration and a smaller heat-affected zone. This is because the laser pulse duration is short for thermal transport and shorter than the thermal relaxation time, resulting in shallow penetration and a smaller heat-affected zone as shown in figure 1.13 (b) leading to improved quality of surface treatment (124, 125).

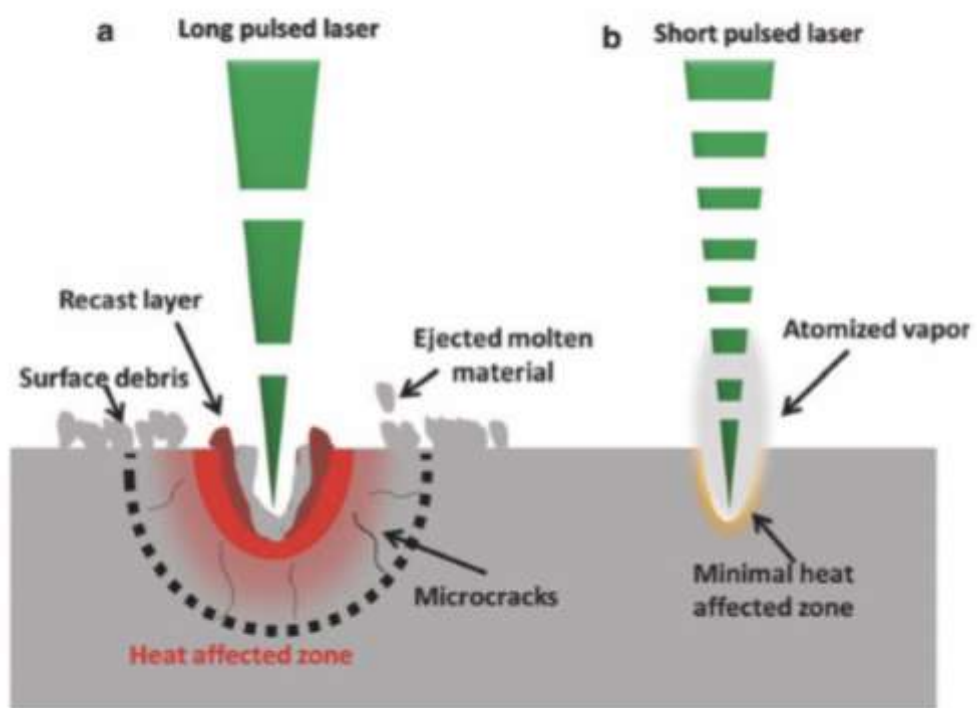


Figure 1.13: Effect of long laser pulses versus short laser pulses (124).

#### 1.14.4 Power density

The power density is correlated with the area of the focused beam and peak power ( $P_p$ ) as shown in the equation:

$$\text{Power density} = P_p / A = W / \text{cm}^2$$



As a result, high laser energy and short duration of laser pulse yield high power density which accelerate the rate of material removal and accordingly lead to reduction of the recast layer (120).

### 1.14.5 Laser frequency

Laser frequency or pulse repetition rate is defined as number of pulses per second (126). Collected data reported that a direct relationship between the surface texturing and frequency value was not found (127, 128), However logical relationship maybe present because changing in laser frequency affecting other parameters that affect the final texturing such energy, peak power, melting volume for every pulse, solidification rate and surface morphology (127).

### 1.14.6 Focusing lens; Focal position and focal length

The two parameters that affect the characteristics of laser treated surface are focal position and focal length, which are related to the distribution of laser power and the spot size onto the surface of material

According to the following equation, the minimum spot size is proportional to focal length.

$$d_f = f \theta$$

Equation where  $d_f$  is the spot diameter,  $f$  is the focal length, and  $\theta$  is the angle of full beam divergence.

The distance over which the changing in focused spot diameter occur by 5% is called the depth of focus which is estimated from the following equation

$$\Delta f = \frac{2df f}{db}$$

Where  $db$  is the unfocused beam diameter.

From the above equation, the longer focal length lens provides deeper depth of focus (figure 1.14) **(112)**.

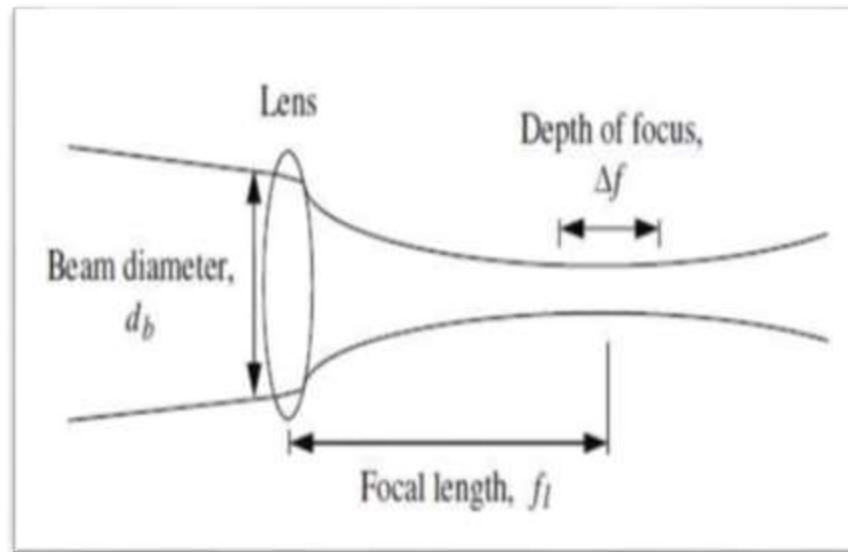


Figure1.14 : Depth of focus **(112)**.

### 1.14.7 Scanning speed (mm/sec)

One of essential parameters during laser- material processing is scanning speed. At a constant spot size and power, changing in scanning speed lead to notable impact on material. In addition to laser power, the scanning speed of the laser beam also affect the power density that induced in the material because at a constant power the increasing in scanning speed lead to reduction in the time of laser material interaction and vice versa **(129)**.

## 1.15 Fiber laser

Fiber laser is a type of solid-state lasers which consist of optical fiber doped by rare-earth elements such as ytterbium (Yb) or erbium. The generation of fiber laser is done by excitation of a rare-earth elements which act as active laser medium within the optical fiber from the ground to the

excited state (population inversion) and stimulated emission of photon in that medium.

Diode laser act as a source of excitation and amplification of light is done along the axis cavity of the resonator by stimulated emission **(130)**.

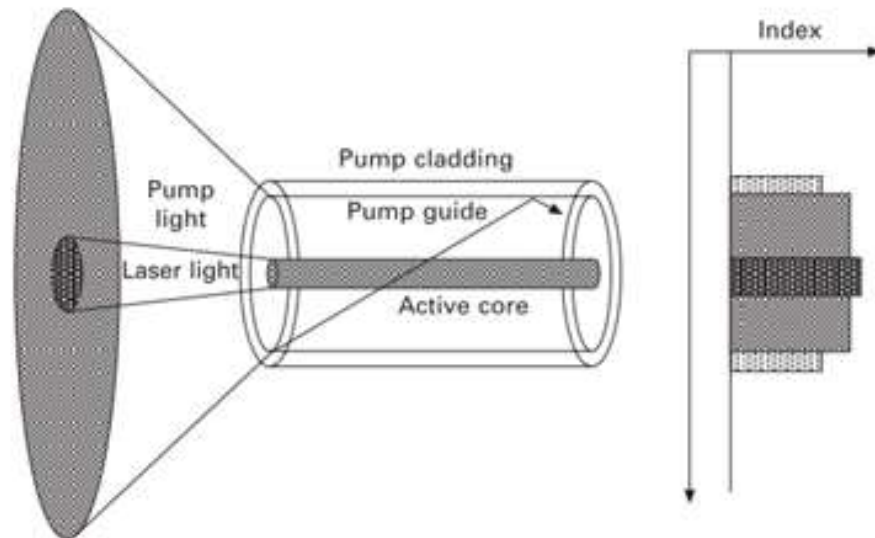


Figure 1.15: Optical fiber of fiber laser **(131)**.

Fiber lasers emit a wider range of wavelength depending on the dopants and they can work either in pulsed mode or continuous wave (CW) **(132)**.

Fiber lasers possesses quick and powerful effect upon surfaces of materials and result in less thermal and mechanical damage compared to other types of laser **(132, 133)**.

Fiber lasers have very high repetition rates which minimize the energy required for ablation, allowing the ablating process to be cooled possible, and increasing the removal process efficacy **(134-136)**.

For diode pumped fiber laser that used in laser beam machining process, Yb doped fiber laser system is used with working wavelength of 1064 nm **(130)**.

## 1.16 Q-switched fiber laser

A Q-switching is one of laser operation modes in which storing of energy is done during pumping in lasing medium as excited atoms and released abruptly in the form of single and short burst. This is obtained by altering the quality factor of laser cavity. The quality factor (Q) is ratio of stored energy in laser cavity to the loss of energy for each cycle **(130)**, the Q-switching method has been widely utilized for fiber lasers in order to obtain pulses with high energy **(137)**.

By this method microsecond or nanosecond pulses are obtained which is extremely preferred for applications that requiring high-energy pulses. This method is cost effective, simple and permit adaptive shaping of pulses **(138)**.

## 1.17 Laser safety

According to their capacity to induce biological damages to the skin or eye, lasers and laser devices are classified into four categories as shown in the table (1.1).

The aim of laser classifications is to alert users of the possible hazards correlated with the laser in relation to accessible emission limits (AEL). These limits are depend on output energy or power of laser, laser wavelengths, exposure duration and the laser beam cross sectional area at the working region **(139)**.

Laser class	Maximum output	Use in dentistry	Possible hazard	Safety measures
Class I Class IM	40 $\mu$ W (blue) 400 $\mu$ W (red)	Integral scanning, laser caries detector	No implicit risk Possible risk with magnified beam	Blink response Laser safety labels
Class II Class IIM	1.0 milliWatt (mW)	Laser caries detection, aiming beams	Possible risk with direct viewing, significant risk with magnified beam (Class IIM)	Sight aversion response Laser safety labels
Class IIIR Class III	Visible 5.0 mW Invisible 2.0 mW 500 mW (0.5 W)	Some low-level lasers, aiming beams Low-level lasers	Eye damage Eye damage – direct or specular, maximum output may pose slight fire/skin risk	Safety eyewear, safety personnel, training for Class IIIR and IIIB lasers
Class IV	No upper limit	All surgical lasers	Eye/skin damage, nontarget tissue fire hazard, plume hazard, possible ionizing effects with UV lasers	Safety eyewear, safety personnel, training/local rules, possible registration with national regulations

Table 1.1: A summary of laser classes, possible hazards and safety measures for lasers that are commonly used in clinical dentistry (139).

## 1.18 Literature review

Table1.2: Literature Review

Author /year	Type of laser	Laser parameters	Test	Conclusion
Ates <i>et al.</i> , 2017 (14)	Ultrafast fiber laser	<ul style="list-style-type: none"> <li>• P<sub>aver</sub>= 20 W</li> <li>• t<sub>p</sub> =100 ns</li> <li>• F= 100 kHz</li> <li>• λ=1064 nm</li> <li>• E= 0.6 mJ</li> <li>• P<sub>p</sub> = 6 kW</li> </ul>	<ul style="list-style-type: none"> <li>• SEM</li> <li>• SBS</li> <li>• surface roughness measurement (Ra) by profilometer</li> <li>• EDS</li> <li>• MOF</li> </ul>	Laser surface treatment increased surface roughness and significantly increase the SBS
Venkat, et al.,2017 (15)	Nd:YAG	<ul style="list-style-type: none"> <li>• t<sub>p</sub>= 3 μs</li> <li>• λ=1064 nm</li> <li>• fluence= 4.0 J/cm<sup>2</sup></li> </ul>	<ul style="list-style-type: none"> <li>• SEM</li> <li>• SBS</li> </ul>	Laser treated surfaces exhibit significant increasing in SBS
Kılıçarslan <i>et al.</i> , 2016 (16)	Nd:YAG	<ul style="list-style-type: none"> <li>• t<sub>p</sub> = 10 ms</li> <li>• λ=1064 nm</li> </ul>	<ul style="list-style-type: none"> <li>• SEM</li> <li>• SBS</li> <li>• surface roughness measurement (Ra) by profilometer</li> <li>• MOF</li> </ul>	the SBS not significantly increased by Nd:YAG laser treatment



## **1.19 Aims of the Study**

The present study aimed to:

1. Assessment of the effect of fiber laser (1064 nm) on surface morphology and surface roughness of titanium discs using optical microscope, surface roughness tester, SEM and XRD.
2. Evaluation of the shear bond strength and the modes of failure between titanium and resin cement after using fiber laser (1064 nm) as a surface treatment method considering different laser parameters.



## **CHAPTER TWO**

### **MATERIALS AND METHODS**

## CHAPTER TWO

This chapter includes materials and equipment, which used in this study; also includes the methods of performing this study, laser system set up, the pilot study, testing methods and the statistical analysis.

### 2.1 List of Materials and equipment

Materials and equipment used in this study were elucidated in (tables 2.1 and 2.2).

Table 2.1: List of the materials

<b>Materials</b>	<b>Company and origin</b>
Breeze self-adhesive resin cement	Pentron, lot no.7770196, USA
Commercially pure titanium grade II rod	Baoji Jinsheng Metal Material/China/ Lot No. JS120316
Distill water	Iraq
Ethanol alcohol	Scharlau, Spain
Self-Cure acrylic powder	Veracril, lot no.AR 23119, Colombia
Self-cure acrylic liquid	Veracril, lot no.MA o3119, Colombia
Silicon carbide paper	Struers, Denmark
Silicon mold (Custom made)	Silect light, Muller –omicron ,Germany

Table 2.2: List of equipment

<b>Equipment</b>	<b>Company and origin</b>
Surface roughness tester	SRT-6210,China
Digital ultrasonic cleaner	CD-7810A/ New Trent, China
Digital Vernier	TOPEX 150 mm /China
Fiber laser	Wuxi Raycus fiber laser Technologies CO.,LTD/RFL-P100Q,China
Lathe cut Machine	Bantam, Italy
LED Light curing device	LED curing light/LY-A180,China
Optical microscope	OLYMPUS/BX51, Korea
Polishing machine	Struers/DAP-7, Denmark
Scanning Electron Microscopy	TESCAN,VEGA II/Republic of Czech
Stereomicroscope	Hamilton microscope,BLS120,Korea
Universal testing machine	LARYEE, WDW-50,50 KN,China
X-ray diffractometer	XRD-6000/SHIMADZU, Japan
Water bath	BS-11/LAB COMPANOIN ,Korea

## **2.2 Methods**

### **2.2.1 Titanium discs preparation**

Titanium discs ( n= 72) were cut from Cp Ti rod grade 2 by wire cut lathe machine into circular discs 6 mm x 3 mm (diameter and height respectively). The grinding of discs and polishing was done by using a grinding and polishing machine rotated at 250 rotations per minute (rpm) with silicon carbide paper in sequence of 120, 320, 500, 800, 1000, 1200, 2000 and 2400 size of grit to obtain a uniform, smooth mirror-like surface.

After that discs were cleansed ultrasonically using ethanol for 15 min followed by distilled water 10 min, for removing of contaminations and

debris (figure 2.2) (99). At last, the discs were set aside for drying at room temperature.



Figure 2.1: Titanium discs.



Figure 2.2: Ultrasonic cleaner.

### 2.2.2 Laser system

A Q-switched nanosecond Ytterbium (Yb) fiber laser that shown in (figure 2.3) was used in this study which has the following specifications:

- a) Laser wavelength: 1064 nm
- b) Average power: up to 104 W
- c) Pulse duration: 81 ns
- d) Beam diameter: 6.6 mm
- e) Frequency: 20-200 kHz



Figure 2.3: Fiber laser

### 2.2.3 Surface roughness measurements

Ra of the samples were measured by surface roughness tester that illustrated in (figure 2.4) The surface roughness tester contain a diamond probe pin with 5  $\mu\text{m}$  radius positioned in orientation perpendicularly to the surface of the sample and 0.25 mm was the level of cut-off. On each sample surface and at a distinct point, three measurements were evaluated after that the average value of Ra for each sample was calculated in  $\mu\text{m}$  (89).

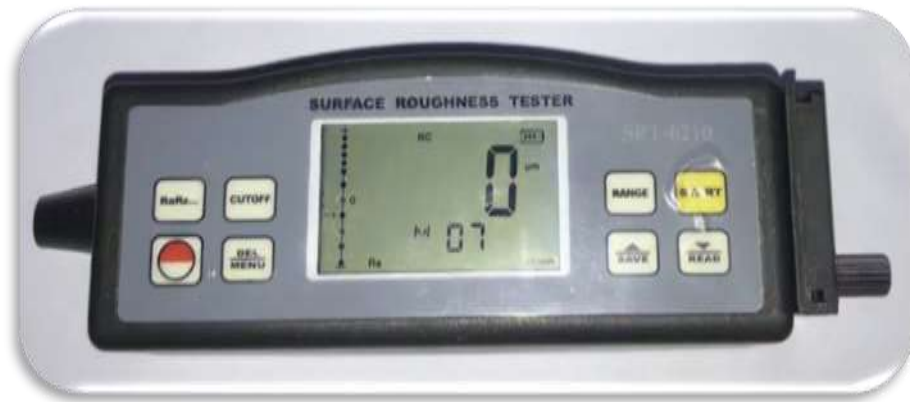


Figure 2.4: Surface roughness tester

### 2.2.4 Phase analysis

Phase analyzing of irradiated titanium samples achieved by X-ray diffraction that illustrated in (figure 2.5), that operate at 30 mA current and 40 kV voltage and scanning range ranged from 10 to 90 degrees along with two theta. Results of XRD pattern were indexed in accordance with ICDD (International Center for Diffraction Data).



Figure 2.5: X-ray diffraction machine.

## 2.2.5 The pilot study

A pilot study (N= 32) was conducted to obtain the most appropriate laser parameters that enhance the roughness of titanium surface devoid of cracks or defects.

### 2.2.5.1 First pilot study group

A first pilot study (n =5) carried out for estimation the appropriate standoff distance between disc surface and laser source. Discs irradiated with 5 W average power, 10000 mm/s scan speed, 20 kHz repetition rate, 0.01 mm spot size and standoff distance was 11.6 cm, 11.7 cm, 11.8 cm, and 11.9 cm (Figure 2.6).The most appropriate standoff distance with no charring evidence is 11.9 cm which remained constant in all experimental group.

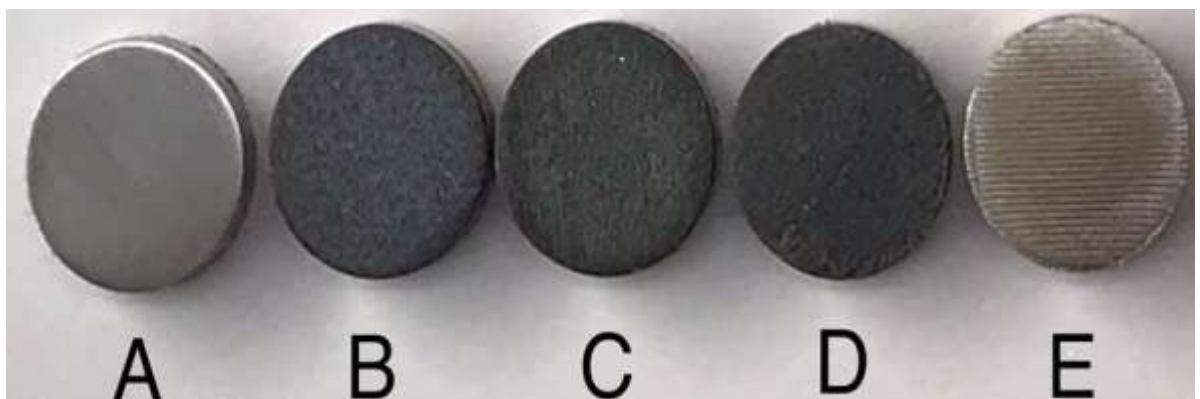


Figure 2.6: (A) Control disc (B-E) discs irradiated with standoff distance values of 11.6, 11.7, 11.8 and 11.9 cm respectively.

### 2.2.5.2 Second pilot study group (hatch spacing variations)

In second pilot study group (n=5) irradiation of titanium discs with fiber laser done with average power of 5 W, speed 10000 mm/s , 0.05 mm spot size and repetition rate of 20 kHz, these parameters remained constant for all samples of this group while hatch spacing variations for samples were 0.001, 0.01, 0.05, 0.1 and 0.15 mm.

After surface treatment by laser, the specimens were tested by:

- Optical microscope for surface morphology assessment.
- Surface roughness measurement for assessment of Ra (average surface roughness) of the samples.

According to Ra measurements and examination by optical microscope, the most appropriate hatch spacing is 0.1 mm and this value has remained constant in all of the other group.

### **2.2.5.3 Third pilot study group (Scan speed variations)**

In third pilot study group (n= 6) irradiation of titanium discs with fiber laser done with average power of 5 W, 0.05 mm spot size, 0.1 mm hatch spacing and repetition rate of 20 kHz, these parameters remained constant for all samples of this group while scan speed variations for samples were 10000, 15000, 20000, 25000, 30000 and 35000 mm/s.

Surface roughness measurement for assessment of (Ra) of the samples was done.

According to Ra measurements, the most appropriate scan speed is 10000 mm/s and this value has remained constant in all of the other group.

### **2.2.5.4 Fourth Pilot Study Group (Frequency variations)**

In fourth pilot study group (n=7) irradiation of titanium discs with fiber laser done with average power of 5 W, 0.05 mm spot size, 0.1 mm hatch spacing and speed 10000 mm/s, these parameter remained constant for all samples of this group while frequency variations for samples were 20, 30, 40, 50, 60, 70 and 80 kHz.

Surface roughness measurement for assessment of (Ra) of the samples was done.



According to Ra measurements, the most appropriate frequency is 30 kHz and this value has remained constant in all of the other group.

#### **2.2.5.5 Fifth pilot study group (Average Power variations)**

In fifth pilot study group (n=10) irradiation of titanium discs with fiber laser done with repetition rate of 30 kHz, 0.05 mm spot size, 0.1 mm hatch spacing and speed 10000 mm/s, these parameters remained constant for all samples of this group while average power variations for samples were 3, 5, 7, 10, 15, 20, 25, 30, 40 and 50 W.

After surface treatment by laser, the specimens were tested by:

- Optical microscope for surface morphology assessment.
- Surface roughness measurement for assessment of (Ra) of the samples.
- Selected specimens were tested by SEM for surface morphology assessment at magnification of 500X, 1000X and 2000X.
- Phase analysis for selected specimens were performed by X-ray diffraction (XRD) to determine if there are changes in crystalline structure of titanium following laser irradiation.
- SBS test was performed for selected specimens (3 W, 5 W, 7 W, 10 W and 20 W) with different surface roughness in order to determine the most suitable laser parameters, three specimens were tested for each of the power values above.

The pilot study results showed that the most appropriate laser parameters according to Ra measurements , SEM and SBS test were (hatch spacing 0.1 mm, scanning speed 10000 mm/sec, frequency 30 kHz and laser power 7 W followed by 5 W and 3 W).

## 2.2.6 Study group

After determining the appropriate laser parameters in the pilot study which are fixed for all specimens in the study group, the study group divided into control group and three subgroups each had 10 specimens with different average power setting (3 W, 5 W and 7 W) as following;

**Control group:** Ten titanium specimens were left without any surface treatment and it considered as a control group.

**Group (A):** Ten titanium specimens were irradiated with fiber laser parameters of hatch spacing 0.1 mm, 10000 mm/s scan speed, spot size of 0.05 mm, frequency 30 kHz , average power 3 W and peak power 1234.5 W.

**Group (B):** Ten titanium specimens were irradiated with fiber laser parameters of hatch spacing 0.1 mm, scan speed 10000 mm/s, spot size 0.05 mm, frequency 30 kHz, average power of 5 W and peak power 2057.6 W.

**Group (C):** Ten titanium specimens were irradiated with fiber laser parameters of hatch spacing 0.1 mm, scan speed 10000 mm/s, spot size 0.05 mm, frequency 30 kHz, average power 7 W and peak power 2880.6 W.

One specimen from each group was tested by optical microscope and SEM for assessment of the surface morphology.

Surface roughness measurement for assessment of (Ra) of the samples performed by surface roughness tester.

## 2.2.7 The experimental work

### 2.2.7.1 Rubber mold construction

A circular silicon rubber mold was constructed by using an alumina mold. The silicon mold had 18 x 4 mm (external diameter and height respectively). In the center of the silicon mold, there was a circular opening of 5 mm in

diameter and 3 mm in height to mold the resin cement. This opening was surrounded by a circular border of 6 x 1 mm (diameter and height respectively) that encounter the titanium disc for fitting the silicon mold over the specimen. A stainless steel ring was used for surrounding the outer border of the silicone mold for handling as shown in (figure 2.7).

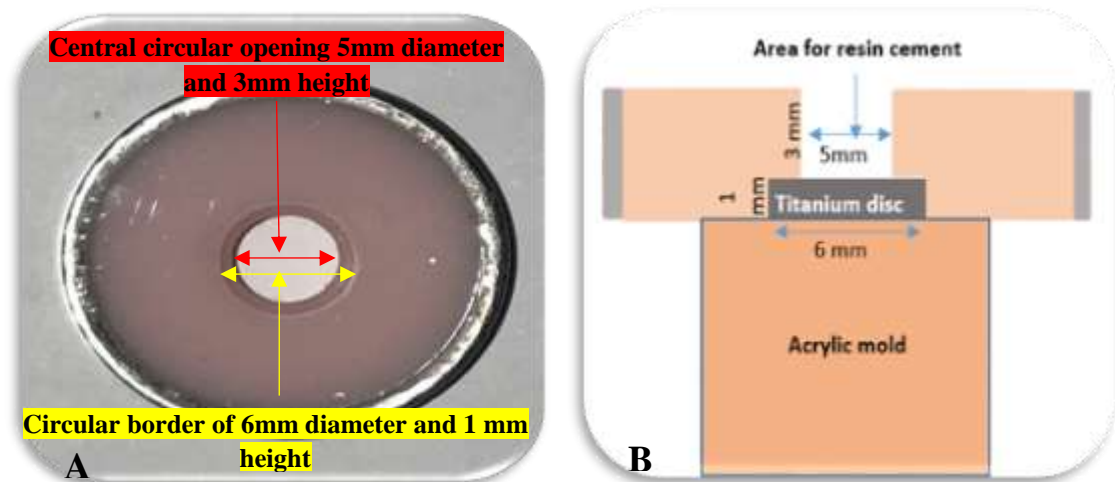


Figure 2.7: (A) Silicone rubber mold (B) cross section of the molded test specimen.

### 2.2.7.2 Cementation procedure

The specimens were horizontally embedded in cold cure acrylic mixing according to manufacturer instruction to about 2 mm in depth and the remaining 1 mm of titanium disc height was left exposed to ensure that the titanium surface remained intact during the bonding procedure with resin cement as shown in (figure 2.8).



Figure 2.8: Acrylic blocks of titanium discs

After that, the silicon mold was precisely fitted over the cylindrical acrylic mold in way that the central opening of the silicon mold positioned on the disc center as shown in (figure 2.9).



Figure 2.9: Positioning of the silicone mold.

After positioning of the silicon mold, the cementation process was performed using self-adhesive resin cement (dual cure) at room temperature (figure 2.10). Adequate amount of resin cement was automixed by using disposable mixing tip (that supplied with the cement kit) and dispensed into the central opening of the silicon mold.



Figure 2.10: Breeze self-adhesive resin cement



Figure 2.11: Cementation procedure over the titanium disc.

Cement excess was removed from the mold periphery by explorer and the resin cement was then photopolymerized with light curing device that shown in (figure 2.12) for 40 sec according to the manufacturer's instructions after that the mold left for 4 minutes to complete the chemical setting.



Figure 2.12: Light curing device

After cementation process, the silicone mold was separated and all discs were stored in water bath contain distilled water for 24 hours duration at 37°C (figure 2.13) prior shear bond strength (SBS) testing (14).



Figure 2.13: Water bath

### 2.2.8 Shear bond strength test

For SBS test, each specimen was placed in the lower jaw of the universal testing machine that illustrated in (figure 2.14), and the stainless steel chisel-

end blade was positioned in a perpendicular position to the interface of titanium and cement as shown in (figure 2.15) and application of load done with 0.5 mm/min speed for cross head till failure occurred (7, 28).

Calculating the Shear stress is done by dividing the applied force by the bonding area that are parallel to the direction of the applied force (26).

SBS values (MPa) were determined following this formulation: (140)

$$S = F/A$$

Where;

S = Shear bond strength [MPa]

F = Applied force [N]

A = bonding area [mm<sup>2</sup>]



Figure 2.14: Universal testing machine



Figure 2.15: Chisel-end blade

### 2.2.9 Modes of failure

After SBS test was performed, the debonded surface of titanium disc was examined by stereomicroscope (figure 2.16) with magnification of (x20) for

determination mode of failure. Mode of failure were categorized as following:(141)

1. Adhesive failure: It take place when resin cement cover less than 25 % of titanium surface.
2. Cohesive failure: It take place when resin cement cover more than 75 % of titanium surface.
3. Mixed failure: This type happened when resin cement cover 25 -75 % of titanium surface.

The percentage of resin cement coverage of titanium surface was measured with image J program.



Figure 2.16: Stereomicroscope

### **2.2.10 Statistical analysis**

Statistical analyzing for Ra and SBS results was accomplished by using “Statistical Package for the Social Sciences” version 24 which include:

I. Descriptive statistics:

- Arithmetic mean.



- Standard deviation “SD”.
- Standard error.
- Maximum and minimum values.
- Statistical tables.
- Graphical representation by bar chart.

## II. Inferential statistics:

- Shapiro-Wilk test was accomplished for testing data normal distribution.
- ANOVA test done to detect significant difference between the means of groups.
- Tukey HSD-test was done to determine the significant difference between every two groups.

Statistical significance of study groups was specified according to the probability value (P) as following:

- a. Significant: when  $P \leq 0.05$ .
- b. Not significant: when  $P > 0.05$ .
- c. Highly significant: when  $P \leq 0.01$

## **CHAPTER THREE**

# **RESULTS, DISCUSSION AND CONCLUSION**

## **CHAPTER THREE**

This chapter include the results of this work, discussion of the obtained results, conclusion and suggestions for the future work.

### **3.1 Results**

#### **3.1.1 Surface morphology**

Surface morphology of titanium discs inspected via optical microscopy and SEM. Optical microscope images (figure 3.1) display irradiated titanium samples with different hatch distance. Photograph of control titanium disc display smoother appearance than those irradiated via fiber laser, in which irradiated discs had texture contain micro-retentive grooves, different degrees of both roughness and hatch distance between adjacent scan paths of laser. Additionally, overlapping was noted between laser scan paths in D1, D2 and D3 samples. No defects or micro cracks were noted.

Selected samples with different average power values as well as control sample were examined by optical microscope and SEM (figures 3.2 – 3.8).

SEM images of laser-irradiated samples exhibited a roughened appearance comparing to control sample. Furthermore, SEM image show a uniform roughness pattern as well as deep laser penetration zones free of defects or cracks even at average power up to 50 W.

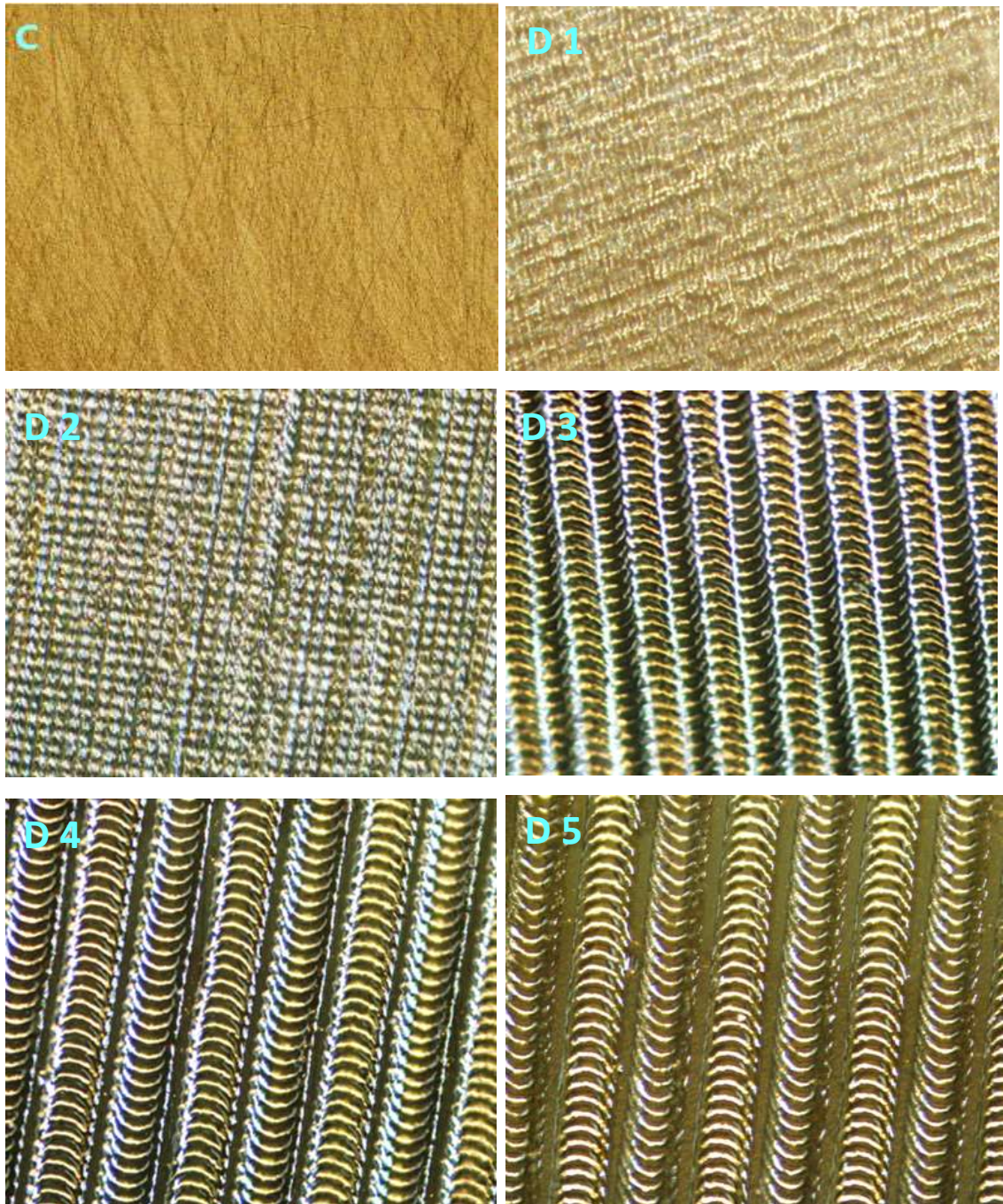


Figure 3.1: Surface morphology images with (X 20) of (C) control, (D1-D5) hatch spacing of 0.001 mm; 0.01 mm; 0.05 mm; 0.1 mm and 0.15 mm respectively.

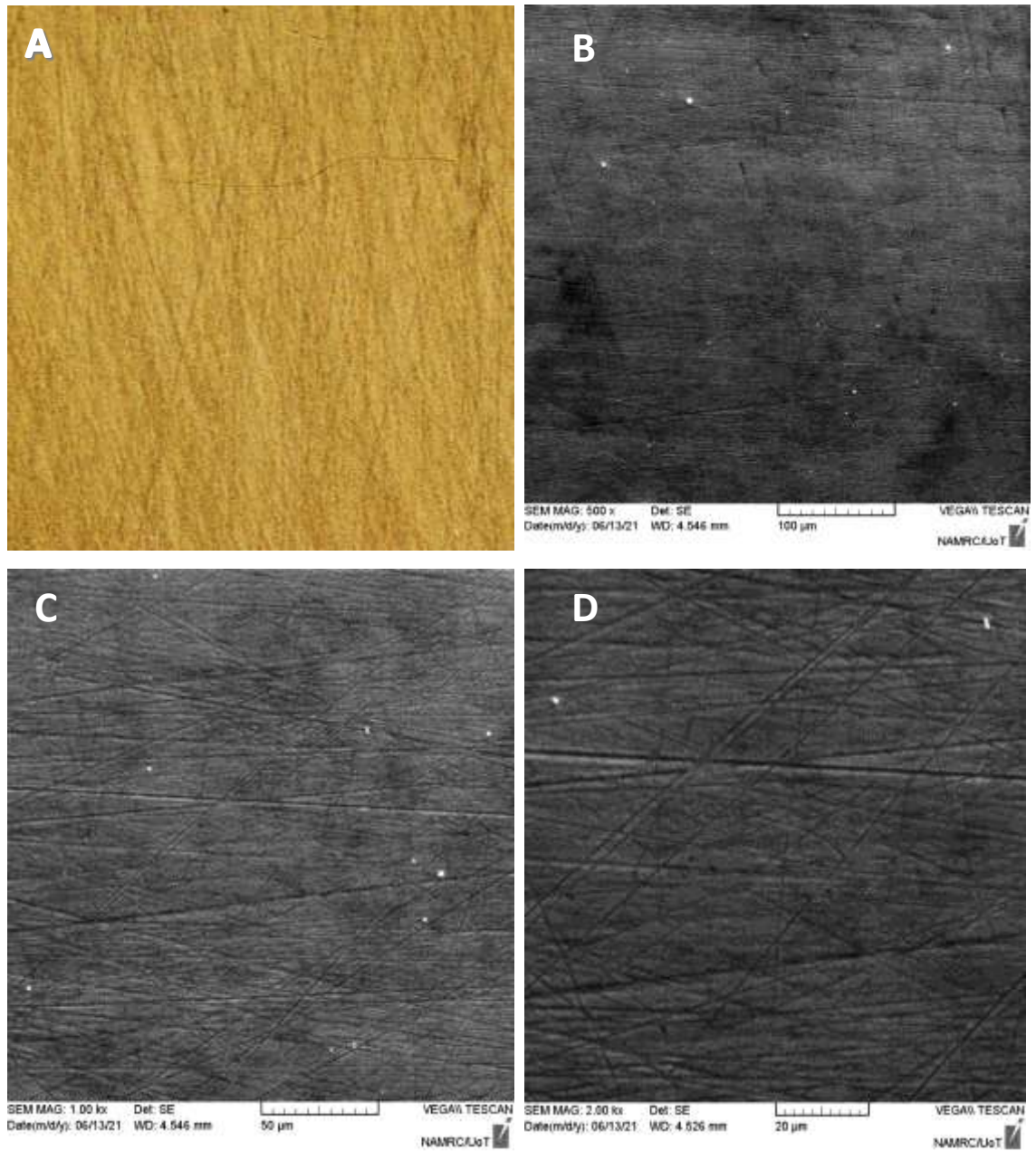


Figure 3.2: Surface morphology of the control specimen. A. Optical microscope (20 X), B. SEM (500 X), C. SEM (1000 X) and D. SEM (2000 X).

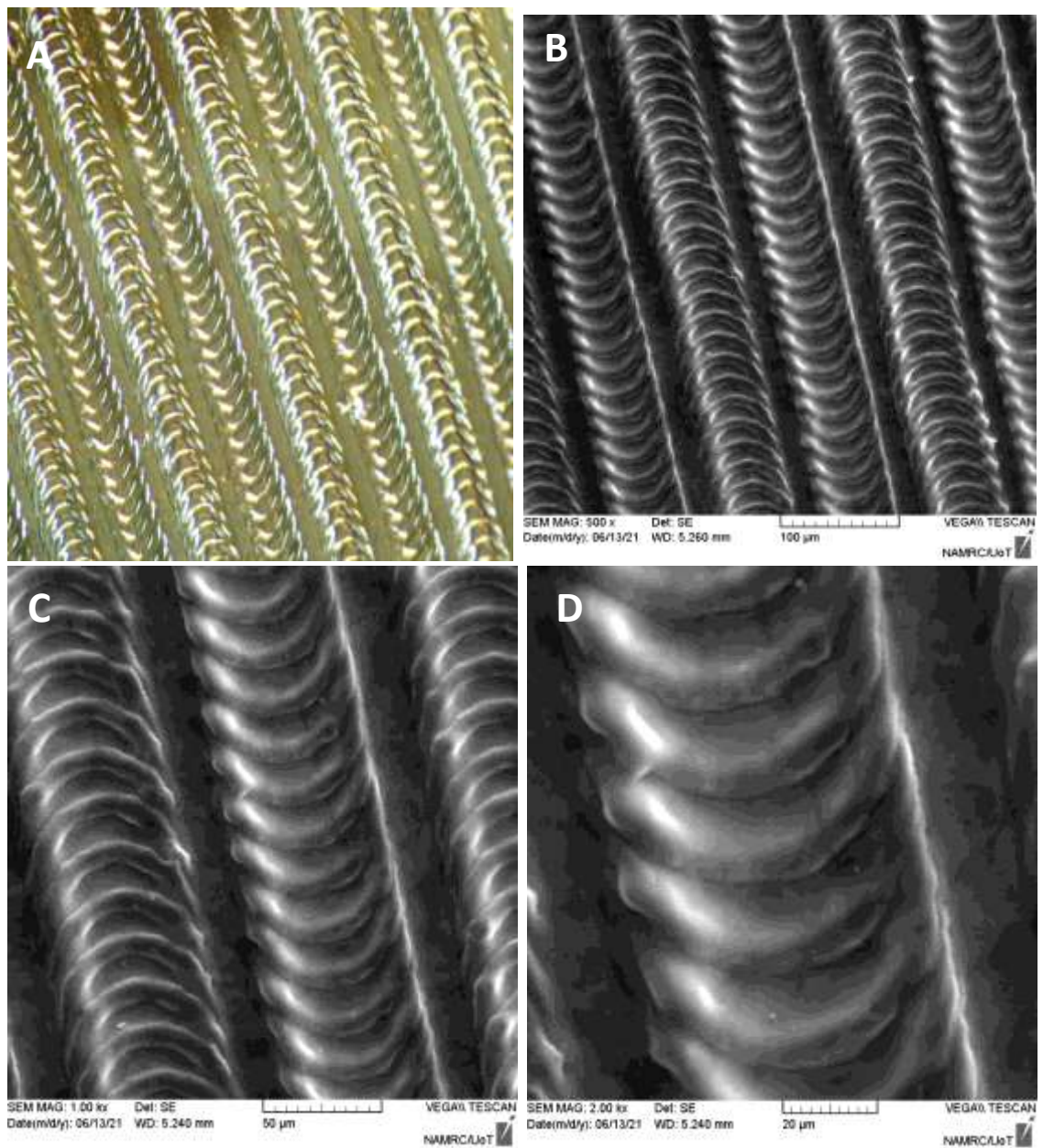


Figure 3.3: surface morphology of irradiated titanium specimen with (average power 3 W, frequency 30 kHz, and scanning speed 10000 mm/sec) (A) Optical microscope (20X), (B-D) SEM with magnifications of 500x, 1000x and 2000x respectively.

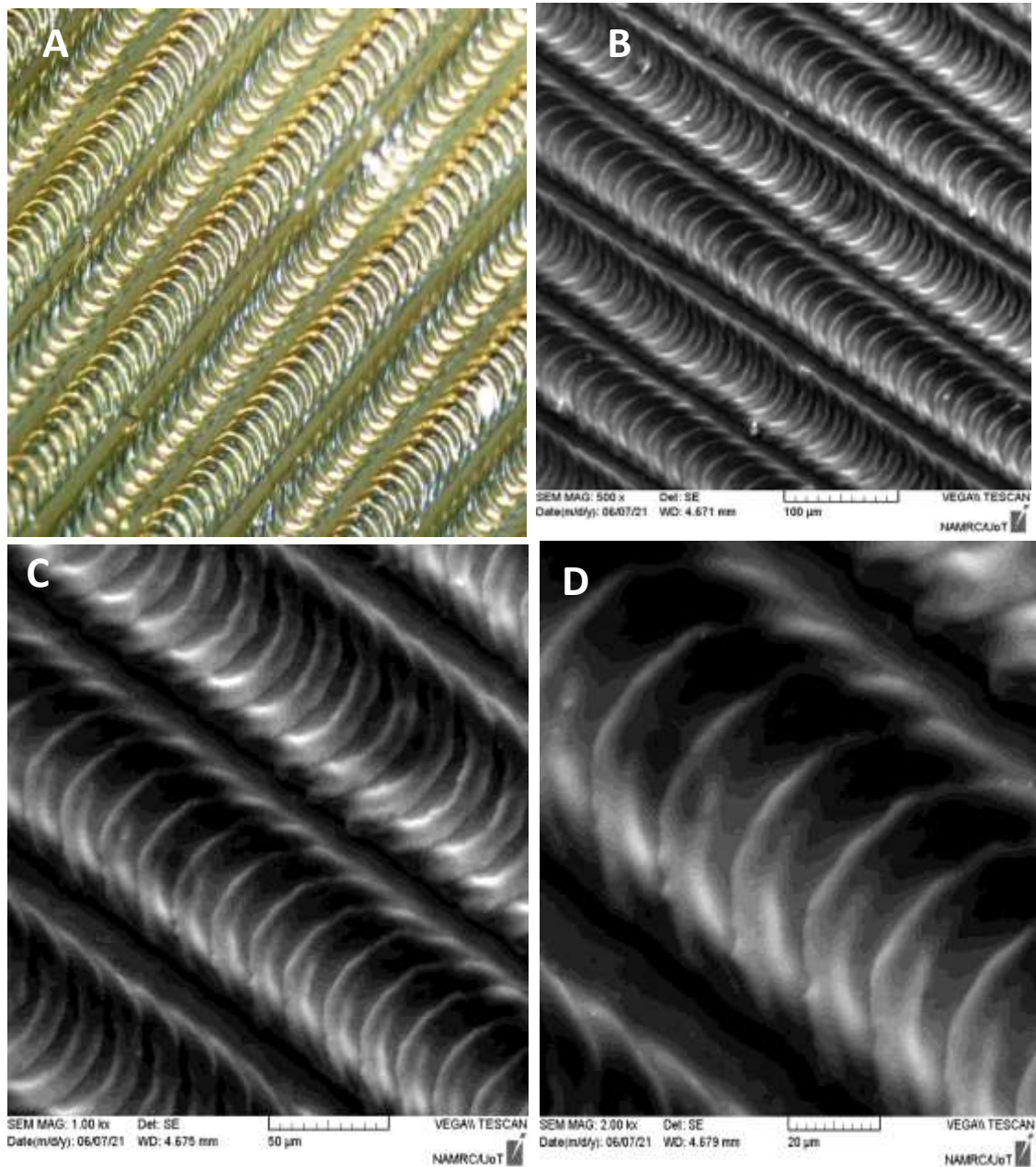


Figure 3.4: Surface morphology of irradiated titanium specimen with (average power 5 W, frequency 30 kHz, and scanning speed 10000 mm/sec) (A) Optical microscope (20X), (B-D) SEM with magnifications of 500x, 1000x and 2000x respectively.

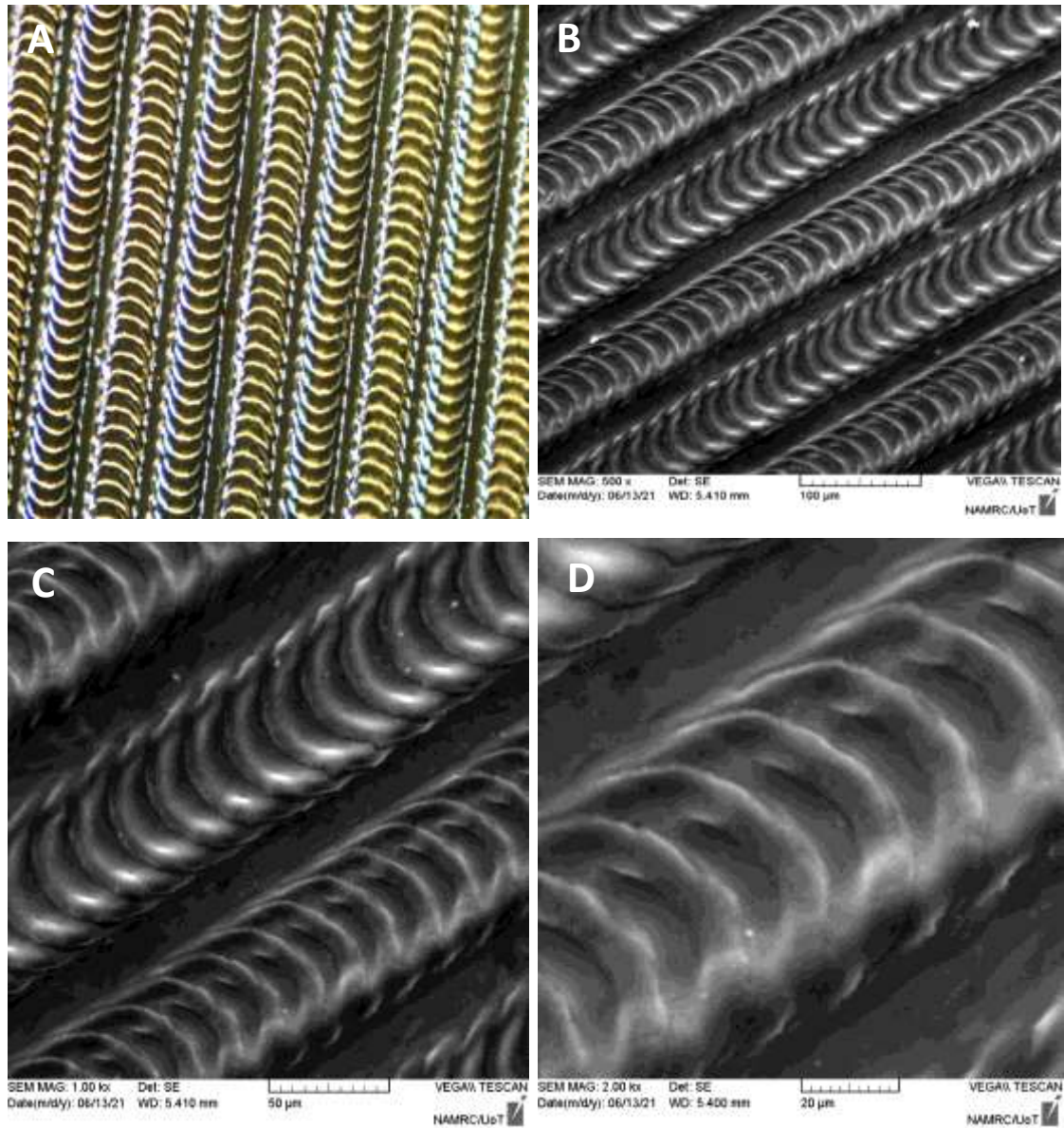


Figure 3.5: Surface morphology of irradiated titanium specimen with (average power 7 W, frequency 30 kHz, and scanning speed 10000 mm/sec) (A) Optical microscope (20X), (B-D) SEM with magnifications of 500x, 1000x and 2000x respectively.



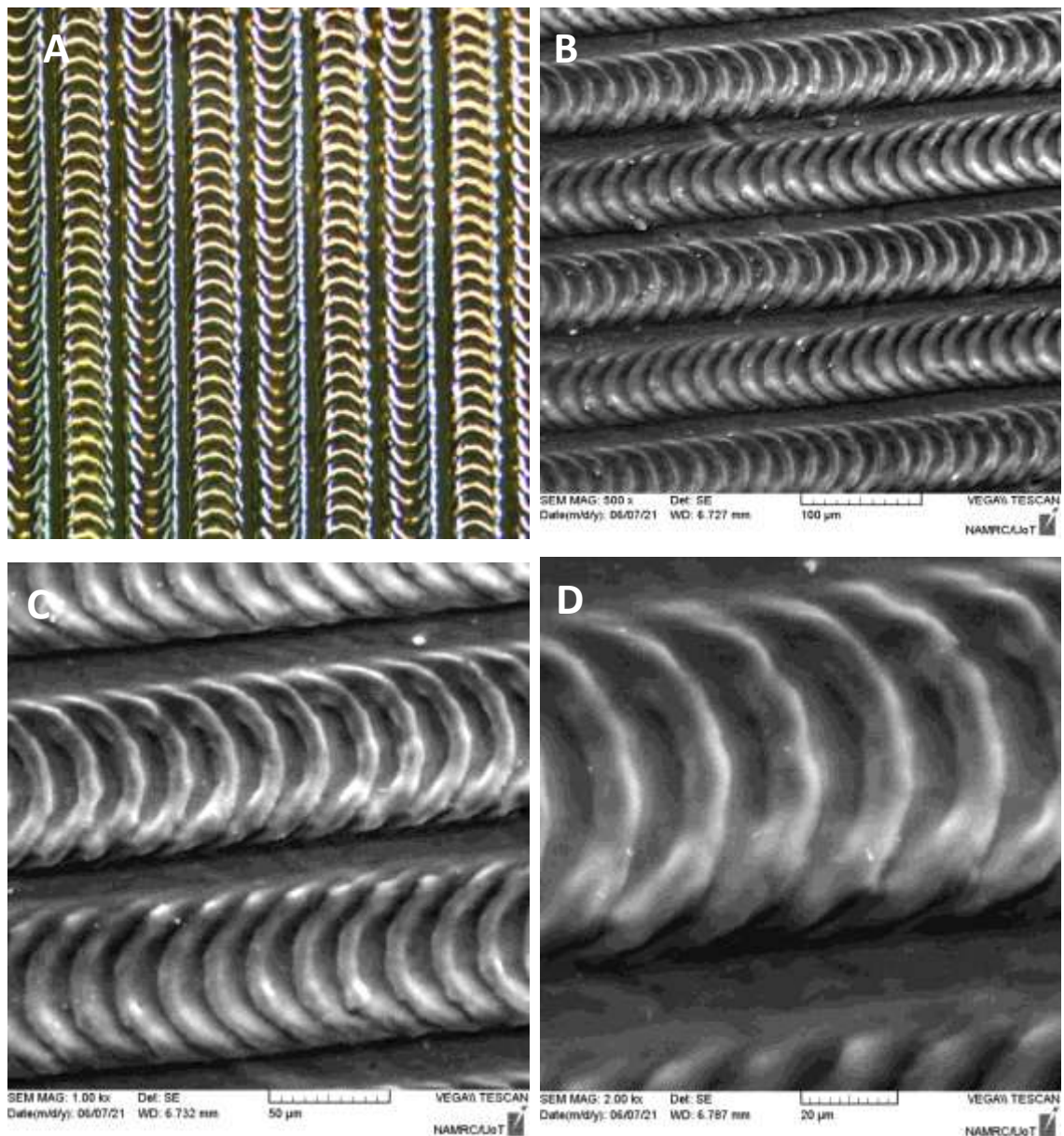


Figure 3.6: Surface morphology of irradiated titanium specimen with (average power 10 W, frequency 30 kHz, and scanning speed 10000 mm/sec) (A) Optical microscope (20X), (B-D) SEM with magnifications of 500x, 1000x and 2000x respectively.

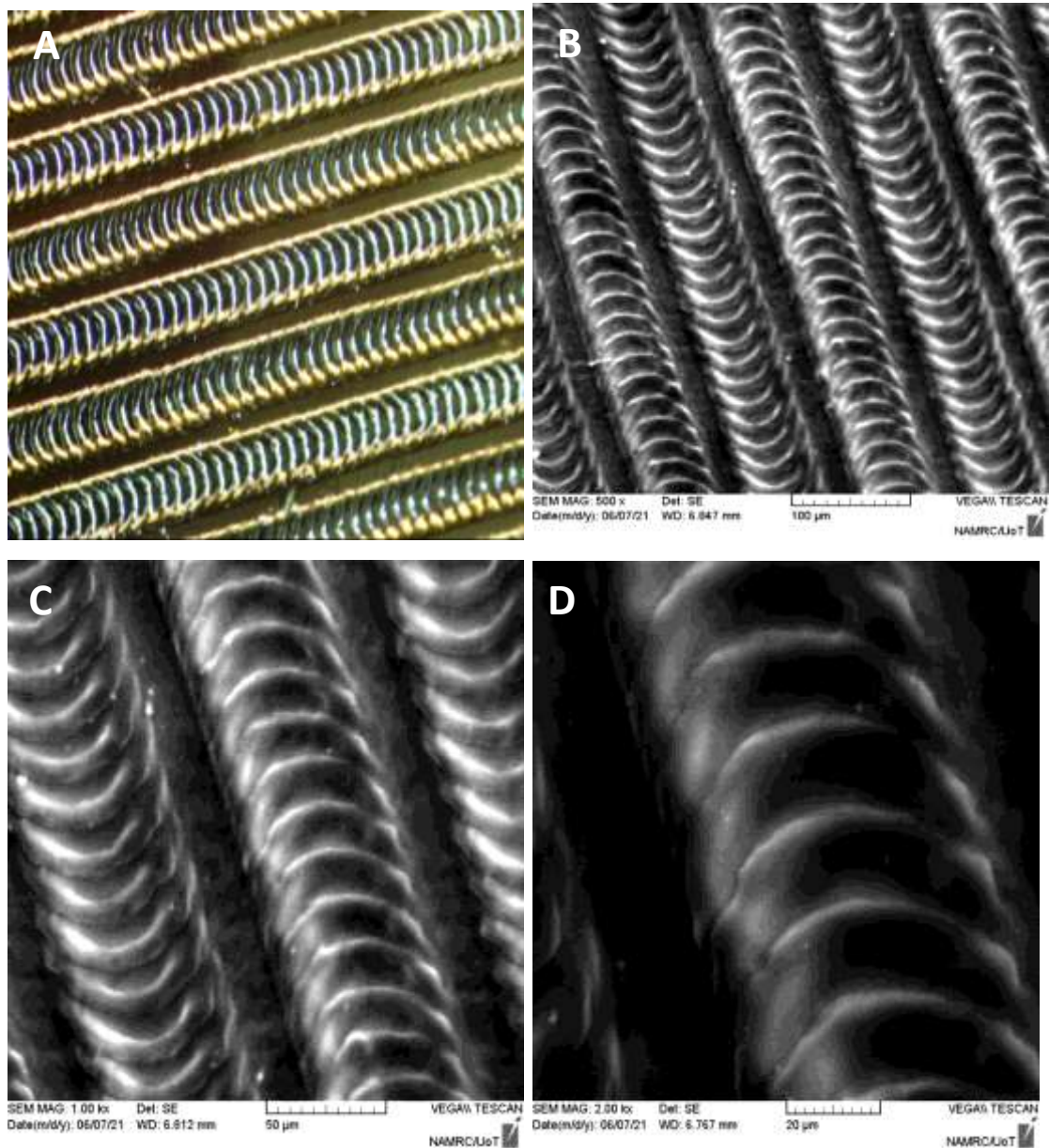


Figure 3.7: Surface morphology of irradiated titanium specimen with (average power 30 W, frequency 30 kHz, and scanning speed 10000 mm/sec) (A) Optical microscope (20X), (B-D) SEM with magnifications of 500x, 1000x and 2000x respectively.

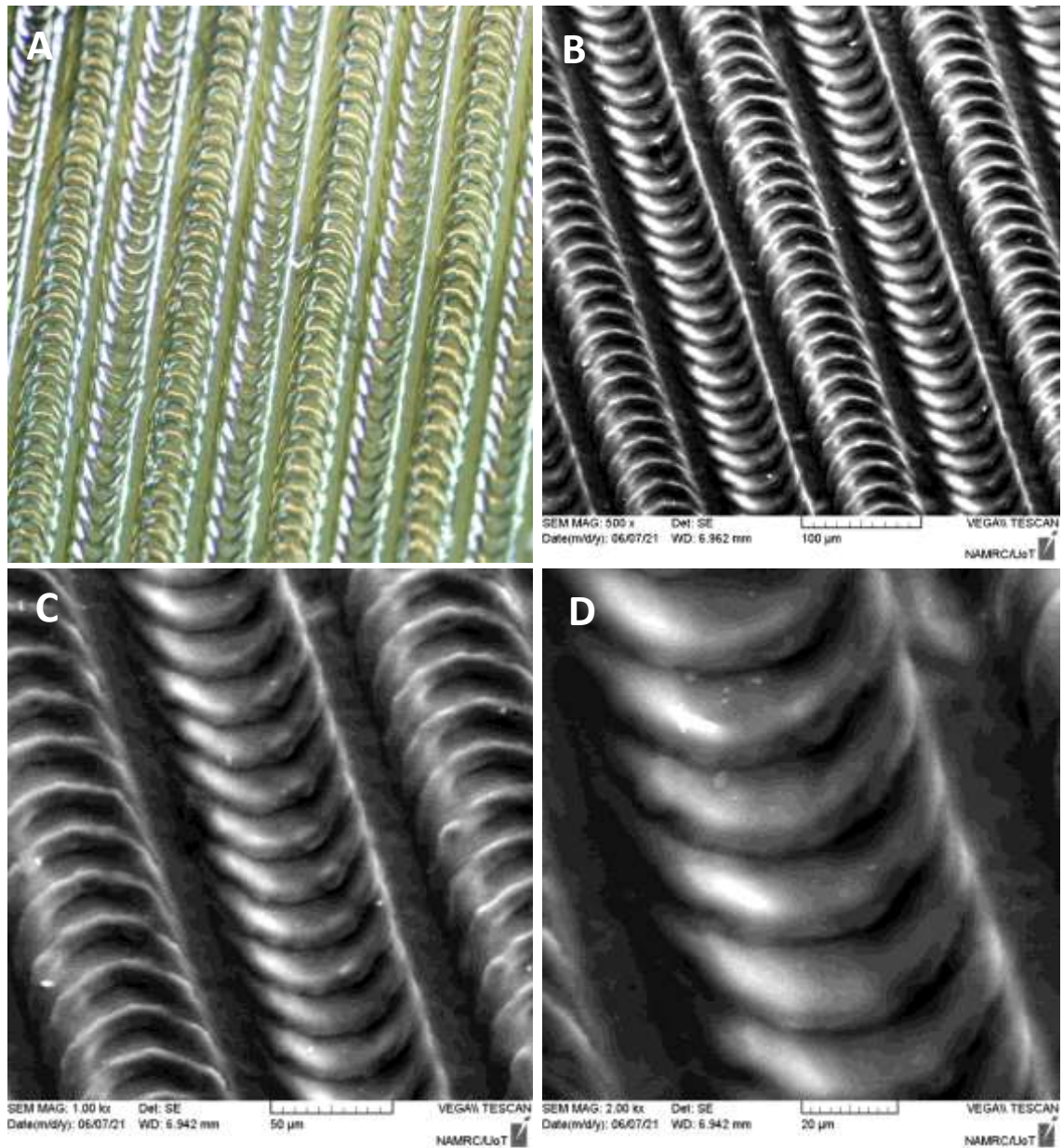


Figure 3.8: Surface morphology of irradiated titanium specimen with (average power 50 W, frequency 30 kHz, and scanning speed 10000 mm/s) (A) Optical microscope (20X), (B-D) SEM with magnifications of 500x, 1000x and 2000x respectively.

### 3.1.2 Surface roughness results

#### 3.1.2.1 Surface roughness results of pilot study

Ra values estimated via surface roughness tester. Lowest value of Ra was noted in control sample ( $0.421\mu\text{m}$ ).

Tables (3.1- 3.4) show Ra of pilot study groups. (Figure 3.9) show Ra of titanium samples as function of laser parameters. Ra at different hatch distance was revealed in figure 3.9 (A). Highest value of Ra was noticed when hatch distance equal to 0.1 mm and lowest value of Ra was noticed when hatch distance equal to 0.001 mm.

Hatch spacing (mm)	Ra ( $\mu\text{m}$ )
0.001	0.653
0.01	1.467
0.05	1.708
0.1	1.951
0.15	1.245

Table 3.1: Ra for the group of hatch distance.

In the group of scanning speed, Ra for different scanning speed were displayed in figure (3.9 B), there is downtrend in Ra value with increased scanning speed.

Scanning speed (mm/sec)	Ra ( $\mu\text{m}$ )
10000	1.951
15000	1.867
20000	1.761
25000	1.708
30000	1.564
35000	1.399

Table 3.2: Ra for scan speed group.

In frequency group, the relation between frequency and Ra were demonstrated in (figure 3.9 C). Maximum value of Ra achieved when frequency equal to 30 kHz.

Frequency (kHz)	Ra ( $\mu\text{m}$ )
20	1.951
30	2.012
40	1.835
50	1.993
60	2.003
70	1.884
80	1.674

Table 3.3: Ra for frequency group.

For the group of average power ,Ra values increased as power increased till it reached to highest value at 10 W , consequently began to decrease up to value of 50 W (figure 3.9 D).

Average power (w)	Ra ( $\mu\text{m}$ )
3	1.533
5	2.012
7	2.321
10	2.359
15	2.319
20	2.304
25	2.259
30	2.213
40	2.176
50	1.964

Table 3.4: Ra for the group of average power.

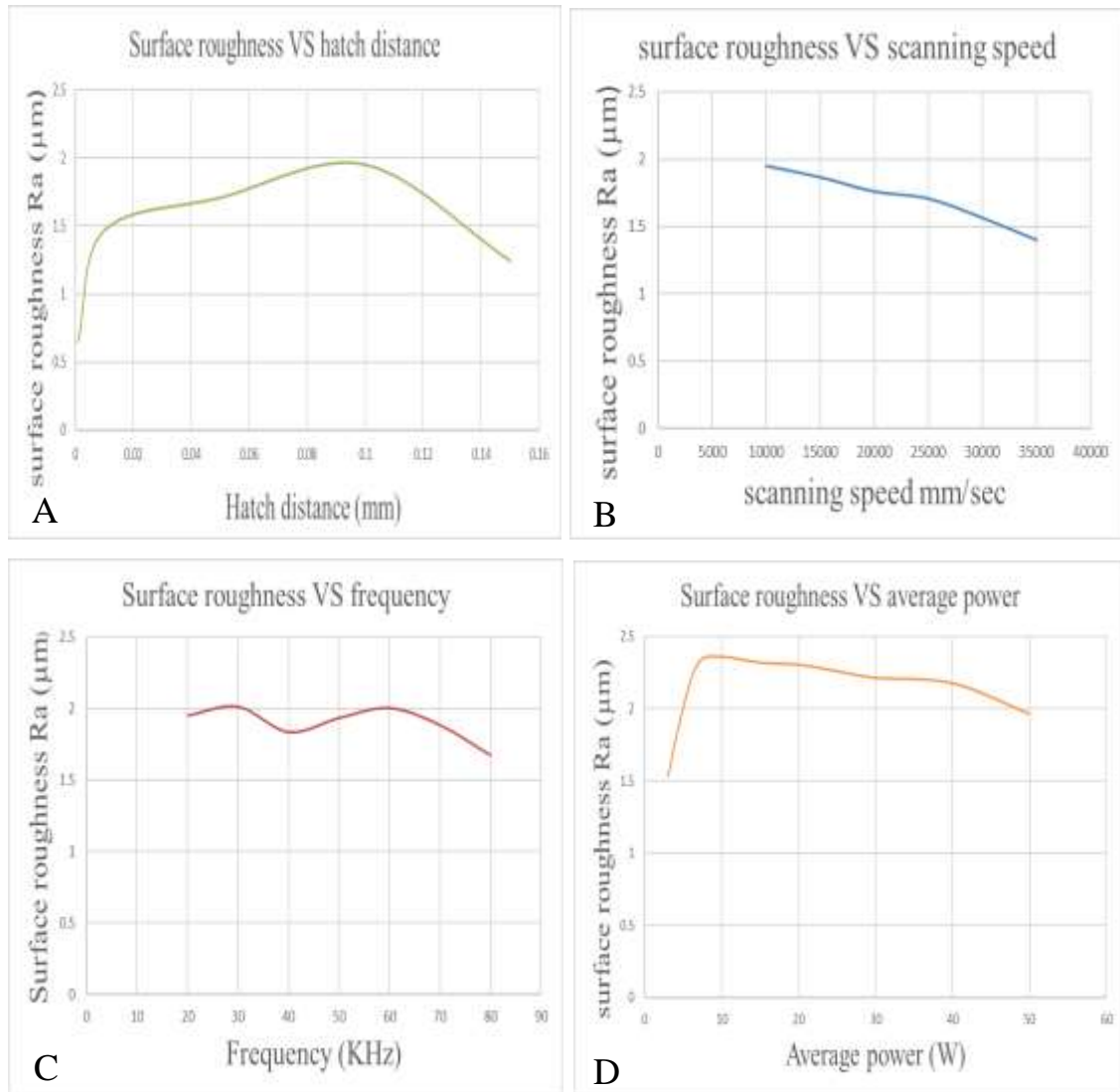


Figure 3.9: Ra for titanium discs as function of laser parameter: (A) hatch distance, (B) scanning speed, (C) frequency and (D) average power.

### 3.1.2.2 Surface roughness results of control and study groups

Average surface roughness (Ra) of the control and study groups was performed by surface roughness tester. (Table 3.5) display the mean and SD of Ra for control and study groups. The highest (Ra) mean obtained from group C (2.33 µm) at average power of 7 W, followed by group B then group C. The lowest (Ra) observed in the control group (0.421 µm).

Groups	N	Mean ( $\mu\text{m}$ )	Std. Deviation	Std. Error	Minimum	Maximum
Control	10	0.421	0.030	.009	0.38	0.47
G (A)	10	1.539	0.017	.005	1.52	1.58
G (B)	10	2.023	0.042	.013	1.98	2.12
G (C)	10	2.330	0.017	.005	2.31	2.36

Table 3.5: Descriptive statistics of the surface roughness for the study group.

Normal data distributions verified by Shapiro-Wilk test as shown in (table 3.6). The results indicated that all data are within normal distribution.

Groups	Shapiro-Wilk		
	Statistic	df	Sig.
Control	.941	10	.566
G (A)	.889	10	.167
G (B)	.865	10	.087
G (C)	.869	10	.096

Table 3.6: Shapiro-Wilk Test of the study Groups.

(Table 3.7) Shows result of ANOVA in which high significant difference was noticed between control and study group.

ANOVA					
Roughness					
	Sum of Squares	df	Mean Square	F	Sig.
Between Groups	21.040	3	7.013	8350.947	0.000
Within Groups	0.030	36	0.001		
Total	21.070	39			

Table 3.7: ANOVA Test of the surface roughness Data.

Results of Tukey in (Table3.8) revealed high significant difference between control and each of study groups besides high significant different was noted among study groups.

(I) Groups	(J) Groups	Mean Difference (I-J)	Significance
Control	G(A)	-1.117	.000
	G(B)	-1.603	.000
	G(C)	-1.908	.000
G(A)	G(B)	-0.486	.000
	G(C)	-0.790	.000
G(B)	G(C)	-0.304	.000

Table 3.8: Tukey Test between the study groups.

### 3.1.3 Analysis of phase

Phase analyzing for selected samples from the group of average power as well as control sample was achieved by XRD. Results of XRD pattern were indexed in accordance with ICDD (International Center for Diffraction Data). There was no change in the phase of titanium following laser treatment as revealed in figures (3.10 and 3.11), this is an essential conditions during Ti treatments. Diffraction peaks corresponded with 100, 002, 101, 102, 110, 103, 200, 112, in addition to 201 were coincided with  $\alpha$ -Ti peaks (hexagonal). Following irradiation with fiber laser, new TiO<sub>2</sub> peaks corresponded with 004 and 301 were noted along with  $\alpha$ -Ti peaks that coincided with anatase TiO<sub>2</sub>.  $\beta$ -Ti, oxynitrides or TiO<sub>2</sub> (rutile) were not determined in any case.



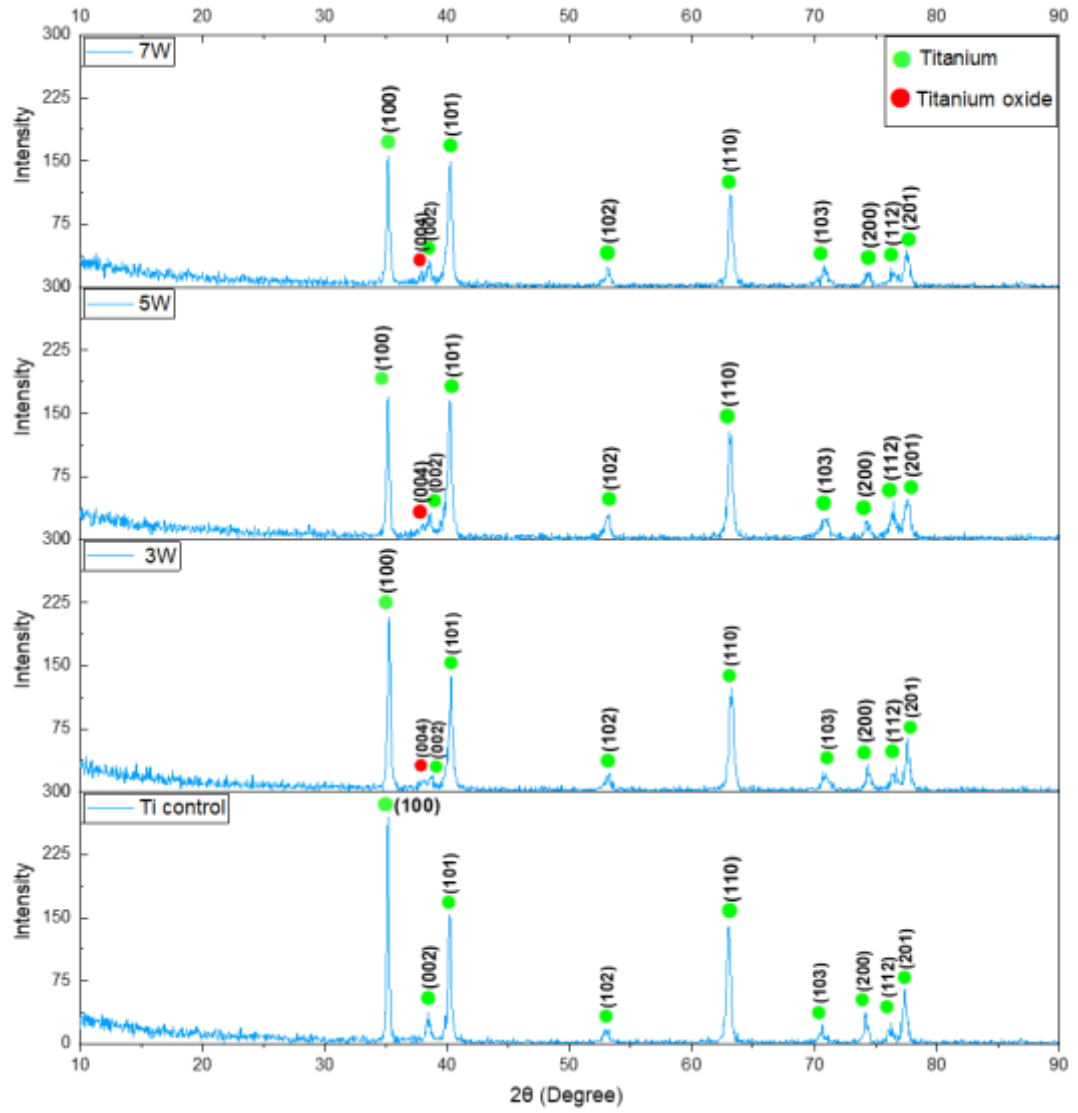


Figure 3.10: XRD patterns of control and (3 W, 5 W, and 7W) laser irradiated specimens.

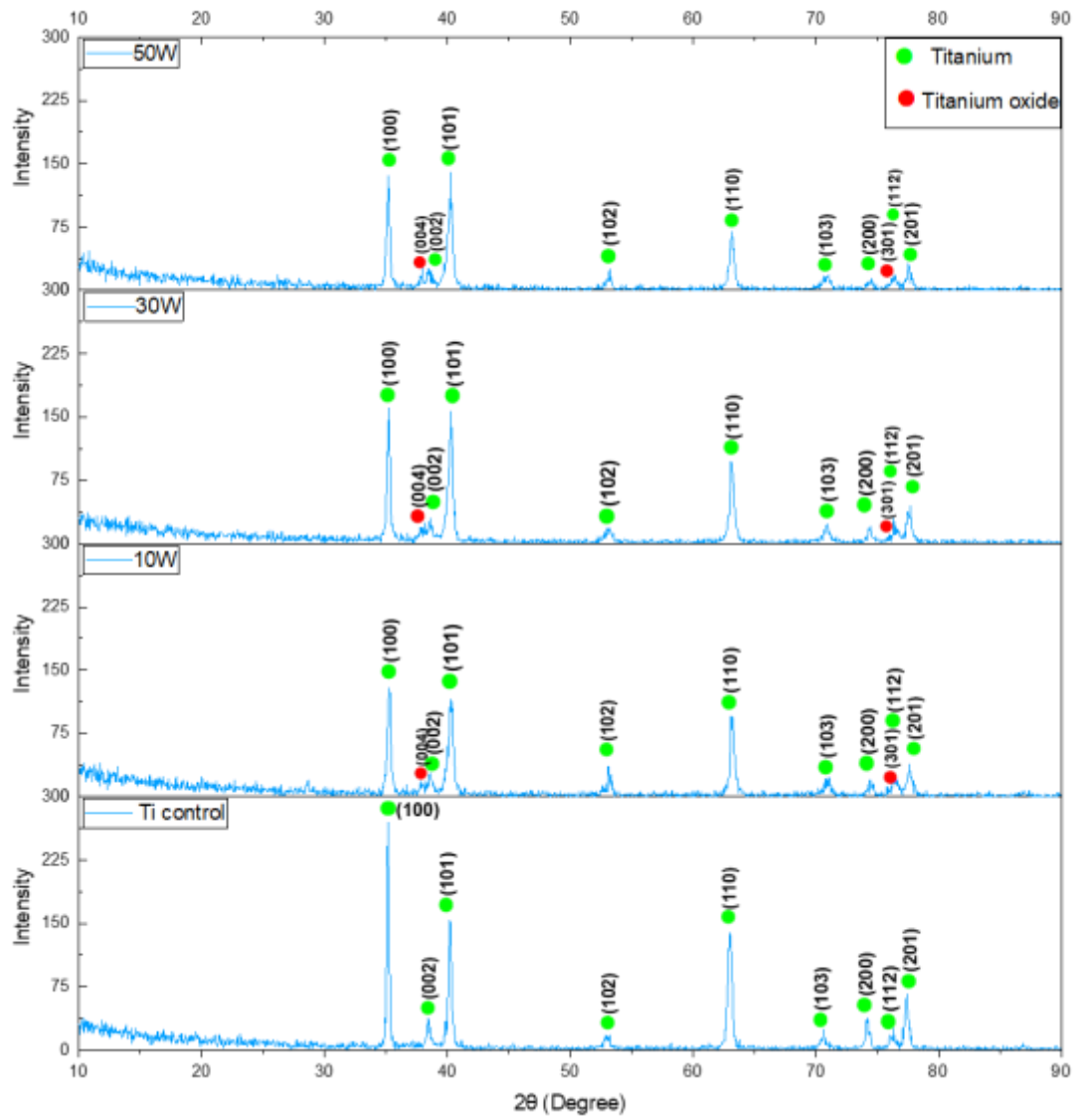


Figure 3.11: XRD patterns of control and (10 W, 30 W, and 50W) laser irradiated specimens.

### 3.1.4 Shear bond strength

#### 3.1.4.1 Shear bond strength of pilot study group

The mean SBS (three specimens for each group) in (Mpa) of the pilot study group are shown in (table 3.9).

The highest SBS mean obtained at average power of 7 W, followed by 20 W ,5 W and then 3 W, while the lowest mean value obtained at average power of 10 W.

Average power (W)	Mean SBS (Mpa)
3	3.903
5	5.820
7	8.030
10	3.834
20	5.983

Table 3.9: Mean SBS of the pilot study groups

#### 3.1.4.2 Shear bond strength of the study group

Mean and SD for SBS test for study groups are shown in (table 3.10).

Group (c) had highest bond strength mean (8.001 MPa) and the control group had the lowest shear bond strength mean (1.585 MPa). (Fig 3.12) shows the bar chart of SBS means for control and study group.

Groups	N	Mean (MPa)	Std. Deviation	Std. Error	Minimum	Maximum
control	10	1.585	.089	.028	1.420	1.680
G (A)	10	3.924	.159	.050	3.710	4.170
G (B)	10	5.819	.166	.052	5.550	6.060
G (C)	10	8.001	.273	.086	7.540	8.450

Table3.10: Descriptive statistic of SBS for the study groups.

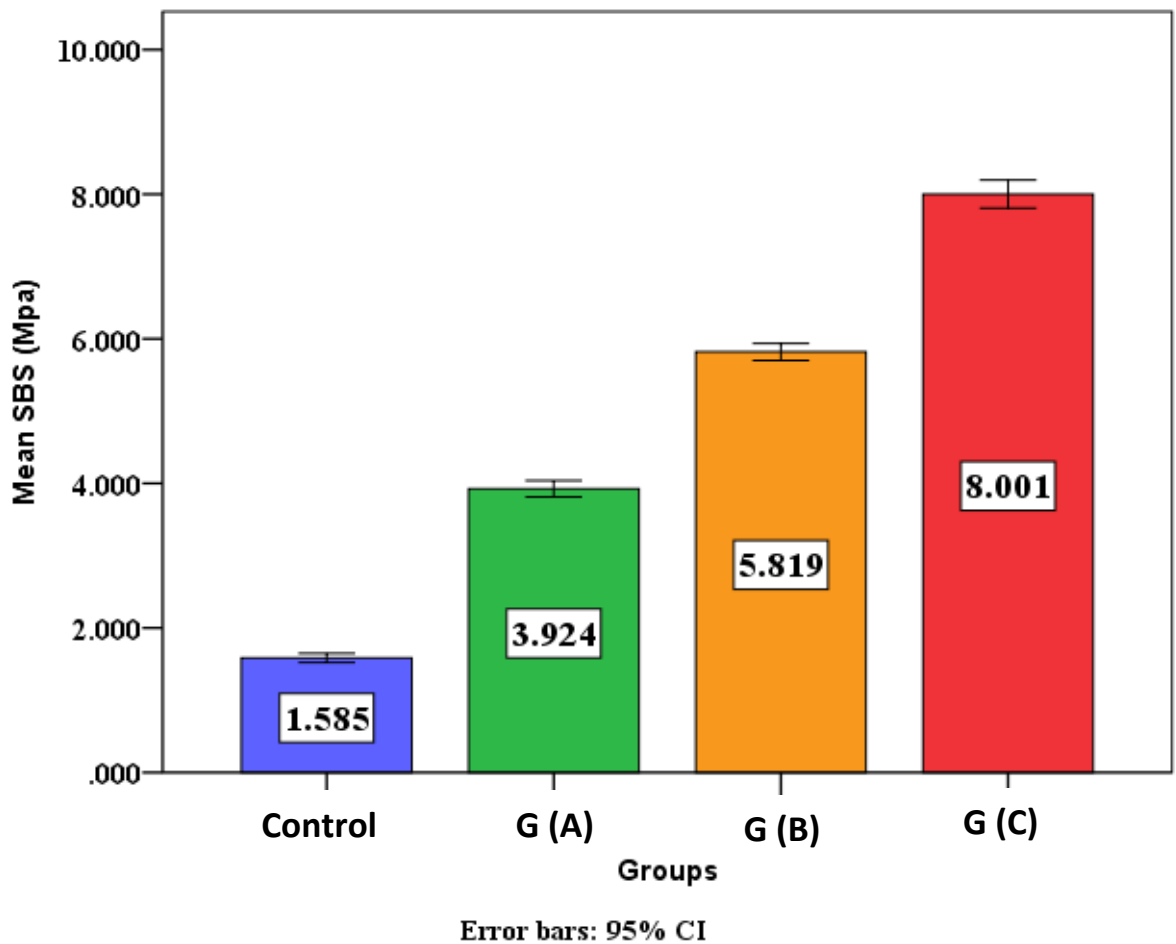


Figure 3.12: bar chart of SBS mean of the study groups.

Shapiro-Wilk test results in (table 3. 11) Indicated that all data are within normal distribution.

Groups	Shapiro-Wilk		
	Statistic	Df	Sig.
Control	.891	10	.176
G (A)	.913	10	.301
G (B)	.963	10	.819
G (C)	.979	10	.958

Table 3.11: Shapiro-Wilk Test of the study Groups.

(Table 3.12) Shows result of ANOVA in which high significant difference was noticed between control and study group.

ANOVA					
SBS (MPa)					
	Sum of Squares	Df	Mean Square	F	Sig.
Between Groups	223.842	3	74.614	2212.843	.000
Within Groups	1.214	36	.034		
Total	225.056	39			

Table 3.12: ANOVA Test of the shear bond strength Data.

Results of Tukey in (Table3.13) revealed high significant difference between control and each of study groups besides high significant different was noted among study groups.

(I) Groups	(J) Groups	Mean Difference (I-J)	Significance
Control	G(A)	-2.339	.000
	G(B)	-4.234	.000
	G(C)	-6.416	.000
G(A)	G(B)	-1.895	.000
	G(C)	-4.077	.000
G(B)	G(C)	-2.182	.000

Table 3.13: Tukey Test between the study groups.

Table 3.14 display the final results of the experimental groups considering different laser parameters, average surface roughness and SBS.

G	Average power (W)	Hatch distance (mm)	Pulse duration (ns)	frequency (kHz)	Scan speed (mm/s)	Ra ( $\mu$ )	SBS (Mpa)
G(A)	3	0.1	81	30	10000	1.539	3.924
G(B)	5	0.1	81	30	10000	2.023	5.819
G(C)	7	0.1	81	30	10000	2.330	8.001

Table 3.14: final results of the experimental groups.

### 3.1.5 Modes of failure

The types of failure for the study groups are shown in (table 3.15) and (figure 3.13). Modes of failure analysis after SBS test showed that the adhesive failure mode was predominant in the control group, the highest frequency of cohesive failure mode was observed in group (C) followed by group (B), while group (A) revealed that the highest mode of failure was mixed mode.(figure 3.14) display stereomicroscope images of modes of failure.

Mode of failure	Control group	Group (A)	Group (B)	Group (C)
Adhesive	90	20	20	10
Cohesive	0	30	40	50
Mixed	10	50	40	40

Table 3.15: Modes of failure for the study groups.

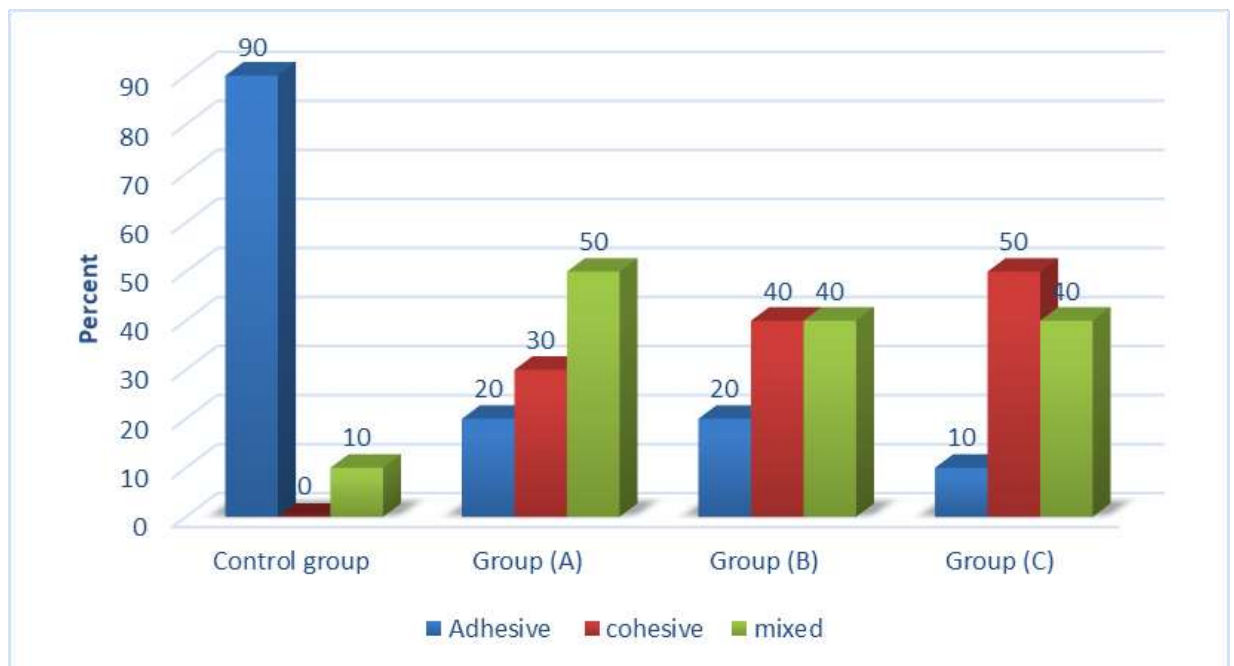


Figure 3.13: Distribution of failure modes in the study groups.

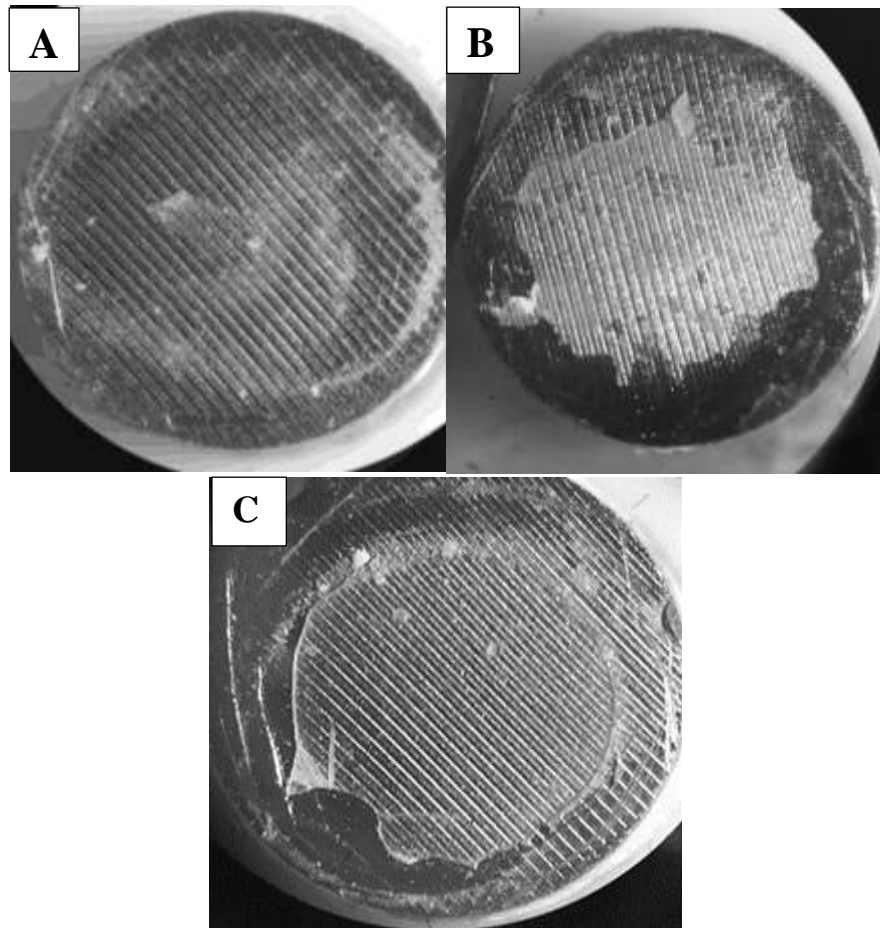


Figure 3.14: Stereomicroscope images of modes of failure (x20) (A) adhesive failure, (B) mixed failure and (C) cohesive failure.



## 3.2 Discussion

Titanium with its exceptional properties and superior biocompatibility has made a noticeable entry in dentistry. Progressively, it has become the preferred material for dental implant. The success of dental implant depending on both the implant itself and the security of retention between the implant abutment and the prosthetic superstructure (15).

The most common complication that associated with cement-retained implant supported prosthesis is retention loss (142). Reliable bonding between titanium abutment and luting cement is essential to guarantee high prosthesis performance.

During laser titanium interaction, absorption is considered the most desirable process because during absorption the optical energy is converted to thermal energy therefore the selection of suitable laser type and parameters to do titanium surface texturings is very important. Parameters of laser have the capacity to modify and change the microstructure of the material surface and enhance the bonding between materials.

Ytterbium doped nanosecond fiber laser emits at wavelength of 1064 nm that appropriate to be absorbed by titanium surface, increases titanium surface roughness, and enhance bonding. On the other hand , fiber lasers have high repetition rates which minimize the energy of pulses required for ablation, allowing the ablation process to be cooled and increasing the removal process efficacy (14, 98). Furthermore , using of fiber laser provides several advantages including predetermining the exact irradiation area by the laser controlling panel with a more homogenous etching pattern can be achieved and there is no need for manual movement of the laser handpiece during texturings as in other laser types.

### 3.2.1 Surface morphology

Surface morphology analysis in the present study has been performed by optical microscope and SEM. The results of the morphological analysis demonstrated that there is variation in surface morphology between control specimens and fiber laser irradiated specimens that resulted from the absorption of laser energy by titanium and conversion of optical energy into thermal energy which might lead to melting and vaporization.

Irradiation of Ti with fiber laser modifies roughness of the surface resulting in an increasing in Ti surface area with no micro cracks or defects even up to average power of 50 W which is an important condition to improve the longevity of implant-supported prosthesis and enhance bonding between implant abutment and cement. The findings of present study corresponded with Korkmaz and Aycan study , who reported that modification of titanium alloy with fiber laser increasing the roughness of the surface with no cracks or defects (98). By comparing this result with the study by Miranda et al., Ustun et al. and Kurt et al. which revealed that irradiation of titanium surface with Er,Cr:YSGG or CO<sub>2</sub> lasers lead to cracks formation (10, 17, 143), the reason for cracks formation might be due to the fact that longer pulse duration resulted in a pronounced heating effect, increased thermal diffusion to the surrounded bulk of material and increased penetration, resulting in high thermal stresses and that inevitably lead to cracks formation (124).

### 3.2.2 Surface roughness (Ra)

Higher values of Ra were noticed in all laser treated samples when compared to control sample. The variations in Ra values among the irradiated samples resulted from variations in the parameters of fiber laser (average power , scan speed , hatch spacing and frequency), that interact with titanium surface leading to different degree of melting and vaporization.

Optimum Ra value achieved at 0.1 mm hatch distance, 30 kHz frequency, 10000 mm/s scan speed and 10 W average power follow by 7 W.

Ra value is in proportion with hatch distance. When the hatch distance increased, Ra value increased but then decreased around 0.15 mm value of hatch distance. The hatch distance represent the distance between two adjacent scan paths of laser, therefore it influence the width of melting volume for the sample (144). As the hatch distance changed, the overlapping area between laser path edges changed and thus affecting the degree of surface roughness. Smaller hatch distance resulted in larger overlapping area, which receive more energy leading to raise the temperature producing wider heat affected zone and increasing the surface melting (145) which in turn lead to reduction in Ra value. Ra value increased progressively with increased hatch distance because of diminished overlapping area and minimized melted volume, however continuous increasing the distance of hatch up to 0.15 mm resulting in a decrease in Ra value because of reduction in melted volume width.

Scan speed is one of essential factors that affects material processing efficiency. In this present study, a reduction in Ra values observed as scan speed increased. Increased scan speed lead to shorter interaction time between laser and material and lower heat impact, this lead to improper surface melting of titanium therefore the Ra value decreased. Furthermore, when average power and frequency values remained constant, the pulse energy also constant and as the speed increased, the number of pulses produced at surface unit line of material decreased, leading to decrease the rate of material interaction because of reduction in pulses overlapping (146).

No direct correlation between Ra and frequency value was observed in the present study. Nevertheless, a logical correlation may be present. Variations in values of frequency have an impact on other parameters, which in turn have an impact on the ultimate surface roughness. At a constant laser average

power, changing the value of frequency can produce changes in energy, peak power, melting volume for every pulse, solidification rate and surface morphology, which have a direct impact on up and down surface fluctuations (roughness) that caused by solidification process (127).

In comparison to average power, scan speed and hatch distance, laser frequency doesn't possess a direct impact on material surface texturing. This observation is consistent with findings by Rafiee et al. as well as Xi et al., they observed that changing the frequency value possess no direct influence on roughness measurements of the surface (127, 146).

A direct association is present between Ra and average power. When average power increased Ra value also increased, however at a certain average power value, Ra decreased because as power increased, energy per each unit area increased and temperature of surface rised leading to melting followed by solidification that lead to enhance surface roughness. Nevertheless, when power rised excessively, the received temperature also rised causing more melting and more melts accumulation on material surface (128), thus Ra value dropped to certain limit.

### 3.2.3 Analysis of phase

Phase analyzing of titanium samples revealed that, there hasn't been any change in phase following treatment with fiber laser. However, Due to the process's performance in an open environment, additional TiO<sub>2</sub> peaks (anatase) were observed in addition to peaks of  $\alpha$ -Ti.

Some elements in air such as O, N and C interact with titanium (147). When oxygen bind with titanium, thin and amorphous oxide layer was created (148, 149). During laser irradiations, Ti surface melted superficially, as a result diffusion of oxygen take place into the molten material causing the Ti surface to oxidize (150). The formation of titanium oxide is very desirable because

it can resist corrosion formation, improving the adhesion properties of titanium and increasing the wear resistance **(151)**.

### **3.2.4 Shear bond strength**

Results of the present study demonstrated that all fiber laser treated groups resulted in highly significant SBS compared with the control group, because the increase in the surface roughness of titanium leading to increase the area of the surface, and surface roughness is considered an important factor in enhancing the bond strength by providing mechanical interlocking favorable by the cement material that enhance the bond strength **(14, 152)**.

The SBS of titanium specimens that were treated with fiber laser (7 W) was higher than the other study groups; this result could be attributed due to the efficacy of fiber laser in roughening the surface of titanium through melting and vaporization processes that result in micromechanical irregularities which increase the mechanical interlocking. Whereas specimens treated with fiber laser at (3 W) displayed the lower SBS among the study groups, this could be attributed to the low average power that was used.

For surface roughness measurement, it was found that SBS value increased with increasing in the surface roughness. However, excessive surface roughness does not enhance the bonding strength. It was found that excessive surface roughness obtained when irradiating the titanium surface with fiber laser at an average power of (10 W) lead to lower SBS value as compared with the study groups, this lead to the fact that excessive roughening of titanium surface doesn't increase the SBS, therefore this group was excluded. Higher surface roughness of titanium forming intense stress locations at the titanium-cement interface in which the sharp angle edges attributed to inadequate flowing of resin cement into the minute irregularities of the surface and prevent the complete bonding of the adhesive with the titanium surface **(98, 153)**, this results is in agreement with some previous studies

which indicated that higher surface roughness doesn't increase the bonding strength (82, 89, 152).

Some studies were conducted for evaluation the effect of laser in enhancing bonding strength between titanium abutment and cement. Ates et al. revealed that irradiation with ultrafast fiber laser lead to increase the surface roughness of titanium and significantly increased the SBS to resin cement and it is considered a substitute method to improve bonding strength (14). Venkat et al. pointed out Nd:YAG laser treatment of titanium abutment enhances the retention of the crown to abutment (15). All of the results of these previous studies are in agreement with this present study.

Conversely, Akın and Güney and reported that laser irradiation of titanium surface with Er:YAG or Nd:YAG lasers did not enhance the bonding strength with resin cement, these controversial results could be explained by laser type or different applied energy and pulse duration (9).

### **3.2.5 Modes of failure**

Essential information related to the bonding quality can be provided by failure modes analysis. In the present study, it was observed that both cohesive and mixed failure types in laser treated groups are higher than the adhesive type and the predominant failure mode in the control group was the adhesive type because the adhesive type could indicate lower bond strength (9, 154), this result is in agreement with Ates et al. study in which the adhesive failure is less in the laser treated group than the control group (14), this means that the bonding strength between laser treated titanium surface and cement is higher than the cohesive strength of the resin cement. Additionally, there was a tendency toward cohesive failure increasing with higher value of bonding strength.

### 3.3 Conclusion

1. Fiber laser parameters are important factors that affect the final results and must be considered during surface treatment.
2. Positive correlation is present between Ra with both hatch distance and average power, and there is negative correlation between Ra and scan speed. However, reduction in Ra values were observed with excessive hatch spacing and average power. There was no obvious correlation between Ra and laser frequency.
3. Fiber laser irradiation of titanium surface increased the bonding surface area without any defects or cracks and enhance the micromechanical retention with the resin cement.
4. Fiber laser irradiation of titanium surface with (frequency of 30 kHz , scan speed of 10000 mm/s, pulse duration of 81 ns, 0.05 mm spot size ,11.9 cm standoff distance and average power of 7 , 5 and 3 W) result in a highly significant increase of shear bond strength with resin cement.

### **3.4 Suggestion for future studies**

1. Future studies are needed applying different lasers types with different parameters and evaluate their effect on surface properties on titanium and SBS to resin cement.
2. Evaluation of other methods for roughness as sandblasting or the effect of metal primer combined with fiber laser on SBS of titanium to resin cement.
3. Evaluation of surface wettability, surface roughness by AFM and matching between particle size of resin cement and roughness of the surface.
4. Investigate the effect of fiber laser 1064 nm on surface properties of other abutment materials and their bonding strength to resin cement.
5. Further studies are needed to evaluate SBS values of laser treated titanium and titanium alloy abutments with different cement types.



# References

## References

1. Shah R, Aras A, Chitre V. Implant-abutment selection: A literature review. *Int J Oral Implantol Clin Res*. 2014;5(2):43-9.
2. Moraschini V, Velloso G, Luz D, Barboza EP. Implant survival rates, marginal bone level changes, and complications in full-mouth rehabilitation with flapless computer-guided surgery: a systematic review and meta-analysis. *International journal of oral and maxillofacial surgery*. 2015;44(7):892-901.
3. Srinivasan M, Meyer S, Mombelli A, Müller F. Dental implants in the elderly population: A systematic review and meta-analysis. *Clinical oral implants research*. 2017;28(8):920-30.
4. Howe M-S, Keys W, Richards D. Long-term (10-year) dental implant survival: A systematic review and sensitivity meta-analysis. *Journal of dentistry*. 2019;84:9-21.
5. Iocca O. *Evidence-Based Implant Dentistry*: Springer International Publishing; 2016.
6. de Oliveira Abi-Rached F, Fonseca RG, Haneda IG, de Almeida-Júnior AA, Adabo GL. The effect of different surface treatments on the shear bond strength of luting cements to titanium. *The Journal of prosthetic dentistry*. 2012;108(6):370-6.
7. Cao Y, Guo Y-y, Chen L, Han J, Tong H, Zhang B, et al. Effects of different surface treatments on bonding strength of resin cement to machined pure titanium. *The journal of adhesive dentistry*. 2019;21(5):401.
8. Sakaguchi RL, Ferracane J, Powers JM. *Craig's Restorative Dental Materials - E-Book*: Elsevier Health Sciences; 2018.
9. Akin H, Guney U. Effect of various surface treatments on the retention properties of titanium to implant restorative cement. *Lasers in medical science*. 2012;27(6):1183-7.

10. Ustun O, Akar T, Kirmali O. A comparative study of laser irradiation versus sandblasting in improving the bond strength of titanium abutments. *Photobiomodulation, photomedicine, and laser surgery*. 2019;37(8):465-72.
11. Sahu N, Lakshmi N, Azhagarasan N, Agnihotri Y, Rajan M, Hariharan R. Comparison of the effect of implant abutment surface modifications on retention of implant-supported restoration with a polymer based cement. *Journal of clinical and diagnostic research: JCDR*. 2014;8(1):239.
12. de Campos TN, Adachi LK, Miashiro K, Yoshida H, Shinkai RS, Neto PT, et al. Effect of surface topography of implant abutments on retention of cemented single-tooth crowns. *The International journal of periodontics & restorative dentistry*. 2010;30(4):409.
13. Kim J-T, Cho S-A. The effects of laser etching on shear bond strength at the titanium ceramic interface. *The Journal of prosthetic dentistry*. 2009;101(2):101-6.
14. Ates SM, Korkmaz FM, Caglar IS, Duymus ZY, Turgut S, Bagis EA. The effect of ultrafast fiber laser application on the bond strength of resin cement to titanium. *Lasers in medical science*. 2017;32(5):1121-9.
15. Venkat G, Krishnan M, Srinivasan S, Balasubramanian M. Evaluation of bond strength between grooved titanium alloy implant abutments and provisional veneering materials after surface treatment of the abutments: An in vitro study. *Contemporary clinical dentistry*. 2017;8(3):395.
16. Kılıçarslan MA, Özkan P, Mumcu E, Deniz ŞT. Efficacy of uncommon surface treatment methods on titanium in order to improve bond strengths for adhesive cementation. *Journal of adhesion science and Technology*. 2016;30(21):2345-56.
17. Kurt M, Külünk T, Ural Ç, Külünk Ş, Danişman Ş, Savaş S. The effect of different surface treatments on cement-retained implant-supported restorations. *Journal of Oral Implantology*. 2013;39(1):44-51.
18. Ferro KJ, Morgano SM, Driscoll CF, Freilich MA, Guckes AD, Knoernschild KL, et al. *The glossary of prosthodontic terms*. 2017.

19. Boemio G, Rizzo P, De Nardo L. Assessment of dental implant stability by means of the electromechanical impedance method. *Smart Materials and Structures*. 2011;20(4):045008.
20. Praveen AS, Arjunan A, Baroutaji A. Coatings for dental applications. 2021.
21. Almas K, Javed F, Smith S. *Glossary of Dental Implantology*: John Wiley & Sons; 2018.
22. Holliday R, Nohl F, Wassell R. *Implant Abutments for Crowns. Extra-Coronal Restorations*: Springer; 2019. p. 231-45.
23. Shafie HR. *Clinical and laboratory manual of dental implant abutments*: John Wiley & Sons; 2014.
24. Özcan M, Hämmerle C. Titanium as a reconstruction and implant material in dentistry: advantages and pitfalls. *Materials*. 2012;5(9):1528-45.
25. Gosavi S, Gosavi S, Alla R. Titanium: A Miracle Metal in Dentistry. *Trends in Biomaterials & Artificial Organs*. 2013;27(1).
26. Phillips RW, Anusavice KJ, Shen C, Rawls H. *Phillips' science of dental materials*: Elsevier/Saunders; 2013.
27. Scarano A, Piattelli M, Vrespa G, Caputi S, Piattelli A. Bacterial adhesion on titanium nitride-coated and uncoated implants: an in vivo human study. *Journal of Oral Implantology*. 2003;29(2):80-5.
28. Veljee TM, Shruthi C, Poojya R. Evaluation and comparison of the effect of different surface treatment modifications on the shear bond strength of a resin cement to titanium: An in vitro study. *The Journal of the Indian Prosthodontic Society*. 2015;15(4):308.
29. Jorge JRP, Barao VA, Delben JA, Faverani LP, Queiroz TP, Assunção WG. Titanium in dentistry: historical development, state of the art and future perspectives. *The Journal of Indian Prosthodontic Society*. 2013;13(2):71-7.
30. Liu X, Chen S, Tsoi JK, Matinlinna JP. Binary titanium alloys as dental implant materials—a review. *Regenerative biomaterials*. 2017;4(5):315-23.

31. Zhang LC, Chen LY. A review on biomedical titanium alloys: recent progress and prospect. *Advanced engineering materials*. 2019;21(4):1801215.
32. Niinomi M, Nakai M. Titanium-based biomaterials for preventing stress shielding between implant devices and bone. *International journal of biomaterials*. 2011;2011.
33. Brown D. All you wanted to know about titanium, but were afraid to ask. *Br Dent J*. 1997;182(10):393-4.
34. W Nicholson J. Titanium alloys for dental implants: A review. *Prosthesis*. 2020;2(2):100-16.
35. Osman RB, Swain MV. A critical review of dental implant materials with an emphasis on titanium versus zirconia. *Materials*. 2015;8(3):932-58.
36. Hisbergues M, Vendeville S, Vendeville P. Zirconia: Established facts and perspectives for a biomaterial in dental implantology. *Journal of Biomedical Materials Research Part B: Applied Biomaterials: An Official Journal of The Society for Biomaterials, The Japanese Society for Biomaterials, and The Australian Society for Biomaterials and the Korean Society for Biomaterials*. 2009;88(2):519-29.
37. Tan PLB, Dunne Jr JT. An esthetic comparison of a metal ceramic crown and cast metal abutment with an all-ceramic crown and zirconia abutment: a clinical report. *The Journal of prosthetic dentistry*. 2004;91(3):215-8.
38. Bidra AS, Rungruanunt P. Clinical outcomes of implant abutments in the anterior region: a systematic review. *Journal of Esthetic and Restorative Dentistry*. 2013;25(3):159-76.
39. Naveau A, Rignon-Bret C, Wulfman C. Zirconia abutments in the anterior region: A systematic review of mechanical and esthetic outcomes. *The Journal of prosthetic dentistry*. 2019;121(5):775-81. e1.
40. Modgi CM, Aras MA. Zirconia abutments in implant dentistry. *Int J Oral Implantol Clin Res*. 2012;3(1):39-42.

41. Mitsias ME, Silva NR, Pines M, Stappert C, Thompson VP. Reliability and fatigue damage modes of zirconia and titanium abutments. *International Journal of Prosthodontics*. 2010;23(1).
42. Foong JK, Judge RB, Palamara JE, Swain MV. Fracture resistance of titanium and zirconia abutments: an in vitro study. *The Journal of prosthetic dentistry*. 2013;109(5):304-12.
43. González D, Cabello G, Olmos G, Niños CL. The saddle connective tissue graft: a periodontal plastic surgery technique to obtain soft tissue coronal gain on immediate implants—a case report. *Int J Esthet Dent*. 2015;10(3):444-55.
44. Montero J, Manzano G, Beltrán D, Lynch CD, Suárez-García M-J, Castillo-Oyagüe R. Clinical evaluation of the incidence of prosthetic complications in implant crowns constructed with UCLA castable abutments. A cohort follow-up study. *Journal of dentistry*. 2012;40(12):1081-9.
45. Alonso-Pérez R, Bartolomé JF, Fraile C, Pradíes G. Original vs Non-Original “Cast-To” Gold Abutment-Implant Connection: Analysis of the Internal Fit and Long-Term Fatigue Performance. 2020.
46. Kim E-S, Shin S-Y. Influence of the implant abutment types and the dynamic loading on initial screw loosening. *The journal of advanced prosthodontics*. 2013;5(1):21-8.
47. Drago C. *Implant Restorations: A Step-by-Step Guide*: Wiley; 2020.
48. Kern M, Lehmann F. Influence of surface conditioning on bonding to polyetheretherketon (PEEK). *Dental Materials*. 2012;28(12):1280-3.
49. Peñarrocha-Diago M, Covani U, Cuadrado L. *Atlas of Immediate Dental Implant Loading*: Springer Nature; 2019.
50. Ortega-Martínez J, Delgado LM, Ortiz-Hernández M, Punset M, Cano-Batalla J, Cayon MR, et al. In vitro assessment of PEEK and titanium implant abutments: Screw loosening and microleakage evaluations under dynamic mechanical testing. *The Journal of Prosthetic Dentistry*. 2020.

51. Evans A, Horton H, Unsworth A, Briscoe A. The influence of nominal stress on wear factors of carbon fibre–reinforced polyetheretherketone (PEEK-OPTIMA® Wear Performance) against zirconia toughened alumina (Biolox® delta ceramic). *Proceedings of the Institution of Mechanical Engineers, Part H: Journal of Engineering in Medicine*. 2014;228(6):587-92.
52. Tetelman ED, Babbush CA. A new transitional abutment for immediate aesthetics and function. *Implant dentistry*. 2008;17(1):51-8.
53. Warreth A, Fesharaki H, McConville R, McReynolds D. An introduction to single implant abutments. *Dental update*. 2013;40(1):7-17.
54. Ma S, Fenton A. Screw-versus cement-retained implant prostheses: a systematic review of prosthodontic maintenance and complications. *International Journal of Prosthodontics*. 2015;28(2).
55. Mehl C, Harder S, Wolfart M, Kern M, Wolfart S. Retrievability of implant-retained crowns following cementation. *Clinical oral implants research*. 2008;19(12):1304-11.
56. Sailer I, Mühlemann S, Zwahlen M, Hämmerle CH, Schneider D. Cemented and screw-retained implant reconstructions: a systematic review of the survival and complication rates. *Clinical oral implants research*. 2012;23:163-201.
57. Vigolo P, Givani A, Majzoub Z, Cordioli G. Cemented versus screw-retained implant-supported single-tooth crowns: a 4-year prospective clinical study. *International Journal of Oral & Maxillofacial Implants*. 2004;19(2).
58. Assenza B, Scarano A, Leghissa G, Carusi G, Thams U, Roman FS, et al. Screw-vs Cement-implant–retained Restorations: An Experimental Study in the Beagle. Part 1. Screw and Abutment Loosening. *Journal of oral Implantology*. 2005;31(5):242-6.
59. Gaddale R, Mishra SK, Chowdhary R. Complications of screw-and cement-retained implant-supported full-arch restorations: A systematic review and meta-analysis. *Int J Oral Implantol*. 2020;13:11-40.

60. Wittneben JG, Joda T, Weber HP, Brägger U. Screw retained vs. cement retained implant-supported fixed dental prosthesis. *Periodontology* 2000. 2017;73(1):141-51.
61. Torrado E, Ercoli C, Al Mardini M, Graser GN, Tallents RH, Cordaro L. A comparison of the porcelain fracture resistance of screw-retained and cement-retained implant-supported metal-ceramic crowns. *The Journal of prosthetic dentistry*. 2004;91(6):532-7.
62. Chee W, Jivraj S. Screw versus cemented implant supported restorations. *British dental journal*. 2006;201(8):501-7.
63. Kendrick S, Wong D. Vertical and horizontal dimensions of implant dentistry: numbers every dentist should know. *Inside Dent*. 2009;4287:2-5.
64. Lee J, Kim Y-S, Kim C-W, Han J-S. Wave analysis of implant screw loosening using an air cylindrical cyclic loading device. *The Journal of prosthetic dentistry*. 2002;88(4):402-8.
65. Kline R, Hoar JE, Beck GH, Hazen R, Resnik RR, Crawford EA. A prospective multicenter clinical investigation of a bone quality-based dental implant system. *Implant dentistry*. 2002;11(3):224-34.
66. Theoharidou A, Petridis HP, Tzannas K, Garefis P. Abutment screw loosening in single-implant restorations: a systematic review. *International Journal Oral & Maxillofacial Implants*. 2008;23(4):681-90.
67. Liang C, Wang W, Pellech T, Suzuki T, Cho S. Change of Sensation Related to Implant Placement: Case Report. *J Oral Bio*. 2016;3(1):4.
68. Tallarico M, Baldini N, Martinolli M, Xhanari E, Kim Y-J, Cervino G, et al. Do the new hydrophilic surface have any influence on early success rate and implant stability during osseointegration period? Four-month preliminary results from a split-mouth, randomized controlled trial. *European journal of dentistry*. 2019;13(01):095-101.
69. El-Helbawy NGE-D, El-Hatery AAE-W, Ahmed MH. Comparison of Oxygen Plasma Treatment and Sandblasting of Titanium Implant-Abutment



Surface on Bond Strength and Surface Topography. *International Journal of Oral & Maxillofacial Implants*. 2016;31(3).

70. Tabakhian G, Nouri A. Effect of different temporary cements on retention of crowns cemented on one piece abutments with two different lengths. *Journal of Mashhad Dental School*. 2012;36(3):223-30.

71. Cano-Batalla J, Soliva-Garriga J, Campillo-Funollet M, Muñoz-Viveros CA, Giner-Tarrida L. Influence of abutment height and surface roughness on in vitro retention of three luting agents. *International Journal of Oral & Maxillofacial Implants*. 2012;27(1).

72. Al Hamad KQ, Al Rashdan BA, Abu-Sitta EH. The effects of height and surface roughness of abutments and the type of cement on bond strength of cement-retained implant restorations. *Clinical oral implants research*. 2011;22(6):638-44.

73. Meshramkar R, Nayak A, Kavlekar A, Nadiger RK, Lekha K. A study to evaluate the effect of taper on retention of straight and angled implant abutment. *Journal of Dental Implants*. 2015;5(1):3.

74. Kim Y, Yamashita J, Shotwell JL, Chong K-H, Wang H-L. The comparison of provisional luting agents and abutment surface roughness on the retention of provisional implant-supported crowns. *The Journal of prosthetic dentistry*. 2006;95(6):450-5.

75. Simon JF, Darnell LA. Considerations for proper selection of dental cements. *Compendium of continuing education in dentistry (Jamesburg, NJ: 1995)*. 2012;33(1):28-30, 2, 4.

76. Sunico-Segarra M, Segarra A. *A Practical Clinical Guide to Resin Cements*: Springer Berlin Heidelberg; 2014.

77. Weiser F, Behr M. Self-adhesive resin cements: a clinical review. *Journal of Prosthodontics*. 2015;24(2):100-8.

78. Vohra F, Al-Rafaiy M, Al Qahtani M. Factors Affecting Resin Polymerization of Bonded All Ceramic Restorations. *Review of Literature*.

- Journal of the Dow University of Health Sciences (JDUHS). 2013;7(2):47-8.
79. Pegoraro TA, da Silva NR, Carvalho RM. Cements for use in esthetic dentistry. *Dental Clinics of North America*. 2007;51(2):453-71.
80. Elsharkawy S, Shakal M, Elshahawy W. Effect of various surface treatments of implant abutment and metal cope fitting surface on their bond strength to provisional resin cement. *Tanta Dental Journal*. 2015;12(4):235-40.
81. Degirmenci K, Saridag S. Effect of different surface treatments on the shear bond strength of luting cements used with implant-supported prosthesis: An in vitro study. *The journal of advanced prosthodontics*. 2020;12(2):75.
82. Seker E, Kilicarslan MA, Deniz ST, Mumcu E, Ozkan P. Effect of atmospheric plasma versus conventional surface treatments on the adhesion capability between self-adhesive resin cement and titanium surface. *The journal of advanced prosthodontics*. 2015;7(3):249-56.
83. Tseng W-Y, Hsu S-H, Huang C-H, Tu Y-C, Tseng S-C, Chen H-L, et al. Low pressure radio-frequency oxygen plasma induced oxidation of titanium–surface characteristics and biological effects. *PLoS One*. 2013;8(12):e84898.
84. Larsson Wexell C, Thomsen P, Aronsson B-O, Tengvall P, Rodahl M, Lausmaa J, et al. Bone response to surface-modified titanium implants: studies on the early tissue response to implants with different surface characteristics. *International Journal of Biomaterials*. 2013;2013.
85. Eliades T, Brantley WA. *Orthodontic applications of biomaterials: A clinical guide*: Woodhead Publishing; 2016.
86. Lim BS, Heo SM, Lee YK, Kim CW. Shear bond strength between titanium alloys and composite resin: Sandblasting versus fluoride-gel treatment. *Journal of Biomedical Materials Research Part B: Applied Biomaterials: An Official Journal of The Society for Biomaterials, The*

- Japanese Society for Biomaterials, and The Australian Society for Biomaterials and the Korean Society for Biomaterials. 2003;64(1):38-43.
87. Pető G, Karacs A, Pászti Z, Guczi L, Divinyi T, Joób A. Surface treatment of screw shaped titanium dental implants by high intensity laser pulses. *Applied Surface Science*. 2002;186(1-4):7-13.
88. Peutzfeldt A, Asmussen E. Distortion of alloy by sandblasting. *American journal of dentistry*. 1996;9(2):65-6.
89. Elsaka SE, Swain MV. Effect of surface treatments on the adhesion of self-adhesive resin cements to titanium. *J Adhes Dent*. 2013;15(1):65-71.
90. Wadhvani C, Chung K-H. Bond strength and interactions of machined titanium-based alloy with dental cements. *The Journal of prosthetic dentistry*. 2015;114(5):660-5.
91. Fonseca RG, Haneda IG, de Almeida-Júnior AA, Abi-Rached FdO, Adabo GL. Efficacy of air-abrasion technique and additional surface treatment at titanium/resin cement interface. *Journal of Adhesive Dentistry*. 2012;14(5).
92. Matinlinna JP, Lassila LV, Vallittu PK. The effect of five silane coupling agents on the bond strength of a luting cement to a silica-coated titanium. *Dental materials*. 2007;23(9):1173-80.
93. Almeida-Júnior AAd, Fonseca RG, Haneda IG, Abi-Rached FdO, Adabo GL. Effect of surface treatments on the bond strength of a resin cement to commercially pure titanium. *Brazilian dental journal*. 2010;21:111-6.
94. Koizuka M, Komine F, Blatz MB, Fushiki R, Taguchi K, Matsumura H. The effect of different surface treatments on the bond strength of a gingiva-colored indirect composite veneering material to three implant framework materials. *Clinical oral implants research*. 2013;24(9):977-84.
95. Bertolotti RL. Adhesion to porcelain and metal. *Dental Clinics of North America*. 2007;51(2):433-51.

96. Ntasi A, Mueller WD, Eliades G, Zinelis S. The effect of Electro Discharge Machining (EDM) on the corrosion resistance of dental alloys. *dental materials*. 2010;26(12):e237-e45.
97. Akin H, Tugut F, Topcuoglu S, Kirmali O. Effects of sandblasting and laser irradiation on shear bond strength of low-fusing porcelain to titanium. *Journal of Adhesive Dentistry*. 2013;15(1).
98. Korkmaz FM, Aycan S. Effect of fiber laser irradiation on the shear bond strength between acrylic resin and titanium. *Scanning*. 2019;2019.
99. Al-Khafaji AM. Assessment of Surface Roughness and Surface Wettability of Laser Structuring Commercial Pure Titanium. *Journal of Research in Medical and Dental Science* 2020;8(1):81-5.
100. Wagner WC. A brief introduction to advanced surface modification technologies. *The Journal of oral implantology*. 1992;18(3):231-5.
101. Gaggl A, Schultes G, Müller W, Kärcher H. Scanning electron microscopical analysis of laser-treated titanium implant surfaces—a comparative study. *Biomaterials*. 2000;21(10):1067-73.
102. Cho S-A, Jung S-K. A removal torque of the laser-treated titanium implants in rabbit tibia. *Biomaterials*. 2003;24(26):4859-63.
103. Linden E, Vitruk P. SuperPulse 10.6 micrometers CO2 laser-assisted, closed flap treatment of peri-implantitis. *Implant Practice US*. 2015;8(4):30-4.
104. Donges A, Noll R. *LASER MEASUREMENT TECHNOLOGY*: Springer; 2016.
105. Avadhanulu M. *An Introduction to Lasers Theory and Applications*: S. Chand Publishing; 2001.
106. Parihar AS. *Contemporary Laser Dentistry*: Notion Press; 2018.
107. Parker S, Convissar R. *Lasers in Restorative Dentistry. Principles and Practice of Laser Dentistry*. New York: Elsevier Inc; 2011.

108. Miserendino LJ, Levy G, Miserendino CA. Laser interaction with biologic tissues. Miserendino LJ, Pick RM Laser in Dentistry Chicago: Quintessence. 1995:39-56.
109. Steen WM, Mazumder J. Laser material processing: springer science & business media; 2010.
110. Yang D. Applications of Laser Ablation: Thin Film Deposition, Nanomaterial Synthesis and Surface Modification: IntechOpen; 2016.
111. Parandoush P, Hossain A. A review of modeling and simulation of laser beam machining. International journal of machine tools and manufacture. 2014;85:135-45.
112. Dahotre NB, Harimkar S. Laser fabrication and machining of materials: Springer Science & Business Media; 2008.
113. Brown MS, Arnold CB. Fundamentals of laser-material interaction and application to multiscale surface modification. Laser precision microfabrication: Springer; 2010. p. 91-120.
114. Salonitis K, Stournaras A, Tsoukantas G, Stavropoulos P, Chryssolouris G. A theoretical and experimental investigation on limitations of pulsed laser drilling. Journal of Materials Processing Technology. 2007;183(1):96-103.
115. Deepa A, Padmanabhan K, Kuppan P. Impact On Structural And Mechanical Properties Of Composites During Machining And Cutting: A Review. J Eng Appl Sci (Asian Res Publ Netw). 2006;11(17):10305-14.
116. Bäuerle D. Laser processing and chemistry: Springer Science & Business Media; 2013.
117. Chaudhary K, Rizvi SZH, Ali J. Laser-induced plasma and its applications. Plasma Science and Technology-Progress in Physical States and Chemical Reactions. 2016:259-91.
118. Majumdar JD, Manna I. Laser-Assisted Fabrication of Materials: Springer Berlin Heidelberg; 2012.
119. Kuar A, Doloi B, Bhattacharyya B. Modelling and analysis of pulsed Nd: YAG laser machining characteristics during micro-drilling of zirconia

- (ZrO<sub>2</sub>). *International Journal of Machine Tools and Manufacture*. 2006;46(12-13):1301-10.
120. Sarfraz S, Shehab E, Salonitis K, editors. A review of technical challenges of laser drilling manufacturing process. *Advances in Manufacturing Technology XXXI: Proceedings of the 15th International Conference on Manufacturing Research*; 2017.
121. Gu DD, Meiners W, Wissenbach K, Poprawe R. Laser additive manufacturing of metallic components: materials, processes and mechanisms. *International materials reviews*. 2012;57(3):133-64.
122. Goodarzi DM, Pekkarinen J, Salminen A. Effect of process parameters in laser cladding on substrate melted areas and the substrate melted shape. *Journal of Laser Applications*. 2015;27(S2):S29201.
123. Ghaini FM, Hamed M, Torkamany M, Sabbaghzadeh J. Weld metal microstructural characteristics in pulsed Nd: YAG laser welding. *Scripta Materialia*. 2007;56(11):955-8.
124. Agrawal R, Wang C. Laser Beam Machining. In: Bhushan B, editor. *Encyclopedia of Nanotechnology*. Dordrecht: Springer Netherlands; 2016. p. 1739-53.
125. Lee W-H, O'zel Tr, editors. Laser micro-machining of spherical and elliptical 3-D objects using hole area modulation method. *International Manufacturing Science and Engineering Conference*; 2007.
126. Convissar RA. *Principles and Practice of Laser Dentistry - E-Book*: Elsevier Health Sciences; 2015.
127. Rafiee K, Naffakh-Moosavy H, Tamjid E. The effect of laser frequency on roughness, microstructure, cell viability and attachment of Ti6Al4V alloy. *Materials Science and Engineering: C*. 2020;109:110637.
128. Xi X, Yongzhi P, Wang P, Fu X. Effect of Laser Processing Parameters on Surface Texture of Ti6Al4V Alloy. *IOP Conference Series: Materials Science and Engineering*. 2019;563:022052.

129. Shukla PP, Lawrence J. *Advances in laser surface treatment of engineering ceramics: viability and characterization techniques*. 2011.
130. Bhattacharyya B, Doloi B. *Machining processes utilizing thermal energy*. *Modern Machining Technology*. 2020:161-363.
131. Denker B, Shklovsky E. *Handbook of solid-state lasers: materials, systems and applications*: Elsevier; 2013.
132. Fornaini C, Poli F, Merigo E, Brulat-Bouchard N, El Gamal A, Rocca J-P, et al. Disilicate dental ceramic surface preparation by 1070 nm fiber laser: Thermal and ultrastructural analysis. *Bioengineering*. 2018;5(1):10.
133. Erdoğan M, Öktem B, Kalaycıoğlu H, Yavaş S, Mukhopadhyay PK, Eken K, et al. Texturing of titanium (Ti6Al4V) medical implant surfaces with MHz-repetition-rate femtosecond and picosecond Yb-doped fiber lasers. *Optics express*. 2011;19(11):10986-96.
134. Aivazi M, hossein Fathi M, Nejatidanesh F, Mortazavi V, Hashemi Beni B, Matinlinna JP, et al. The evaluation of prepared microgroove pattern by femtosecond laser on alumina-zirconia nano-composite for endosseous dental implant application. *Lasers in medical science*. 2016;31(9):1873-43.
135. Kerse C, Kalaycıoğlu Lu H, Elahi P, Çetin B, Kesim DK, Akçaalan Ö, et al. Ablation-cooled material removal with ultrafast bursts of pulses. *Nature* 2016;537(7618):84-8.
136. García-Sanz V, Paredes-Gallardo V, Bellot-Arcís C, Mendoza-Yero O, Doñate-Buendía C, Montero J, et al. Effects of femtosecond laser and other surface treatments on the bond strength of metallic and ceramic orthodontic brackets to zirconia. *PLoS One*. 2017;12(10):e0186796.
137. Vu K, Malinowski A, Richardson D, Ghiringhelli F, Hickey L, Zervas M. Adaptive pulse shape control in a diode-seeded nanosecond fiber MOPA system. *Optics Express*. 2006;14(23):10996-1001.
138. Shi W, Fang Q, Zhu X, Norwood RA, Peyghambarian N. *Fiber lasers and their applications*. *Applied optics*. 2014;53(28):6554-68.

139. Coluzzi DJ, Parker SP. *Lasers in dentistry—current concepts*: Springer; 2017.
140. Murthy V, Manoharan B, Livingstone D. Effect of four surface treatment methods on the shear bond strength of resin cement to zirconia ceramics—a comparative in vitro study. *Journal of clinical and diagnostic research: JCDR*. 2014;8(9):ZC65.
141. Abdulsatar AM, Hussein BM, Mahmood AM. Effects of Different Laser Treatments on Some Properties of the Zirconia-Porcelain Interface. *Journal of Lasers in Medical Sciences*. 2021;12.
142. Chaar M, Att W, Strub J. Prosthetic outcome of cement-retained implant-supported fixed dental restorations: a systematic review. *Journal of oral rehabilitation*. 2011;38(9):697-711.
143. Miranda PV, Rodrigues JA, Blay A, Shibli JA, Cassoni A. Surface alterations of zirconia and titanium substrates after Er, Cr: YSGG irradiation. *Lasers in medical science*. 2015;30(1):43-8.
144. Greco S, Gutzeit K, Hotz H, Kirsch B, Aurich JC. Selective laser melting (SLM) of AISI 316L—impact of laser power, layer thickness, and hatch spacing on roughness, density, and microhardness at constant input energy density. *The International Journal of Advanced Manufacturing Technology*. 2020;108:1551-62.
145. Tian Y, Tomus D, Rometsch P, Wu X. Influences of processing parameters on surface roughness of Hastelloy X produced by selective laser melting. *Additive Manufacturing*. 2017;13:103-12.
146. Xi X, Pan Y, Wang P, Fu X, editors. *Effect of Laser Processing Parameters on Surface Texture of Ti6Al4V Alloy*. IOP Conference Series: Materials Science and Engineering; 2019: IOP Publishing.
147. Hsu S-h, Liu B-S, Lin W-H, Chiang H-C, Huang S-C, Cheng S-S. Characterization and biocompatibility of a titanium dental implant with a laser irradiated and dual-acid etched surface. *Bio-medical materials and engineering*. 2007;17(1):53-68.



148. Park J-H, Heo S-J, Koak J-Y, Kim S-K, Han C-H, Lee J-H. Effects of laser irradiation on machined and anodized titanium disks. *International Journal of Oral & Maxillofacial Implants*. 2012;27(2).
149. Al-Khafaji AMS. Laser Surface Structuring and Coating of Titanium Implant with High Performance Poly Ether Ketone Ketone Polymer (In vitro - In vivo) Study. A PhD thesis, College of Dentistry, University of Baghdad. 2020.
150. Hao L, Lawrence J. Laser surface treatment of bio-implant materials: Wiley Sussex, UK; 2005.
151. Bussoli M, Desai T, Batani D, Gakovic B, Trtica M. Nd: YAG laser interaction with titanium implant surfaces for medical applications. *Radiation Effects & Defects in Solids*. 2008;163(4-6):349-56.
152. Elsaka SE. Effect of surface pretreatments on the bonding strength and durability of self-adhesive resin cements to machined titanium. *The Journal of prosthetic dentistry*. 2013;109(2):113-20.
153. Fawzy AS, El-Askary FS. Effect acidic and alkaline/heat treatments on the bond strength of different luting cements to commercially pure titanium. *Journal of dentistry*. 2009;37(4):255-63.
154. Toledano M, Osorio R, Osorio E, Aguilera FS, Yamauti M, Pashley DH, et al. Durability of resin–dentin bonds: effects of direct/indirect exposure and storage media. *Dental Materials*. 2007;23(7):885-92.

## الخلاصة

**المقدمة:** يعتبر الاستبقاء بين دعامة الزرع والأسمنت المصنوع من الراتنج أحد العوامل الرئيسية التي تساهم في إطالة عمر الترميمات المدعومة بالزرع ؛ يتأثر هذا الاستبقاء بعدة عوامل بما في ذلك خصائص السطح مثل مساحة السطح وخشونة السطح . يمكن إجراء تعديل سطح دعامة الزرع بعدة طرق مثل السفع الرملي والشحذ والحفر بالحامض والمعالجة بالليزر. مع التقدم التكنولوجي ، تم استخدام الليزر لتعديل سطح التيتانيوم لأنها عالية الكفاءة وسهلة الاستخدام.

**الهدف من الدراسة:** التحقيق في تأثير معاملات المعالجة بليزر الايتريبيوم الليفي (المسافة بين الضربات ، وسرعة المسح ، والتردد ومتوسط الطاقة) على خشونة سطح التيتانيوم المستخدمة كدعامة لتعزيز قوة رابطة القص مع الاسمنت الراتنج.

**المواد والطرق:** تم تصنيف أربعين قرصًا من التيتانيوم بحجم 6 مم × 3 مم (قطر وسمك على التوالي) إلى أربع مجموعات (ن = 10) على النحو التالي: مجموعة تحكم بدون أي معالجة سطحية ، المجموعة (ا) تطبيق الليزر الليفي مع متوسط طاقة 3 واط ، ومدة نبضة 81 نانوثانية ، ومسافة توقف 11.9 سم ، وحجم موضع الليزر 0.05 مم ، ومعدل تكرار 30 كيلوهرتز ، وسرعة مسح تبلغ 10000 مم / ثانية ، المجموعة (ب) تطبيق ليزر ليفي بمتوسط 5 واط الطاقة ، ومدة النبضة 81 نانوثانية ، ومسافة التوقف 11.9 سم ، وحجم موضع الليزر 0.05 مم ، ومعدل التكرار 30 كيلوهرتز ، وسرعة المسح 10000 مم / ثانية ، المجموعة (ج) تطبيق ليزر الألياف بمتوسط طاقة 7 واط 81 نانوثانية مدة النبضة ، مسافة التوقف 11.9 سم ، حجم موضع الليزر 0.05 مم ، معدل التكرار 30 كيلو هرتز ، وسرعة المسح 10000 مم / ثانية. تم عمل دراسة تجريبية لتقدير أفضل معايير الليزر. تم إجراء توصيف أقراص التيتانيوم بواسطة المجهر الضوئي ، ومجهر المسح الإلكتروني ، واختبار خشونة السطح. تم إجراء تحليل الطور باستخدام مقياس حيود الأشعة السينية. بعد هذه الاختبارات ، تم تطبيق إسمنت الراتنج على أقراص التيتانيوم باتباع تعليمات الشركة المصنعة. تم تحديد قيم قوة رابطة القص و بعد عملية الفصل ، تم فحص أسطح أقراص التيتانيوم بواسطة مجهر ضوئي لتحديد نوع الكسر. تم إجراء تحليل البيانات احصائيا عن طريق برنامج التحليل المختص.

**النتائج:** لوحظت تغيرات إيجابية في الشكل السطحي لجميع المجموعات التجريبية. لوحظت أعلى قيمة لخشونة السطح في المجموعة (ج) تليها (ب) و (ا) وكانت أقل خشونة للسطح في مجموعة التحكم. تم الحصول على أقل قيمة لقوة ارتباط القص من المجموعة المتحكم وأعلى قيمة لقوة ارتباط القص تم الحصول عليها من مجموعة (ج) تليها (ب) و (ا) بالإضافة إلى ذلك ، هناك تحسن في أنماط الفشل في جميع المجموعات التجريبية. لم يكن هناك تغيير في طور التيتانيوم بعد العلاج بالليزر.

**الاستنتاج:** أظهرت الدراسة الحالية أن المعالجة بالليزر الليفي لسطح التيتانيوم مع (تردد 30 كيلو هرتز ، وسرعة مسح 10000 مم / ثانية ، ومدة نبضة 81 نانوثانية ، وحجم بقعة 0.05 مم ، ومسافة توقف 11.9 سم ومتوسط قوة 7 و 5 و 3 واط) يؤدي إلى زيادة كبيرة في مقاومة القص مع الأسمنت الراتنج.



جمهورية العراق  
وزارة التعليم العالي والبحث العلمي  
جامعة بغداد  
معهد الليزر للدراسات العليا



## تأثير ليزر الإيتربيوم الليفي على ربط دعامة زراعة الأسنان المصنوعة من مادة التيتانيوم والمثبتة بأسمنت الراتنج

رسالة مقدمة الى جامعة بغداد / معهد الليزر للدراسات العليا / لاستكمال متطلبات  
نيل شهادة ماجستير علوم في الليزر/طب الاسنان

من قبل

ربي حسام عبد الرزاق

بكالوريوس طب و جراحة الفم والاسنان – 2012

اشراف

الاستاذ المساعد الدكتورة باسمة محمد علي حسين